

# Collider Probes of Dark Energy Microphysics

Chaitanya Bashyam,<sup>1</sup> Alfredo Gurrola,<sup>1</sup> Andrés Flórez,<sup>2</sup> Cristian Rodríguez<sup>2</sup>  
<sup>1</sup>*Department of Physics and Astronomy, Vanderbilt University, Nashville, TN, USA*  
<sup>2</sup>*Department of Physics, Universidad de los Andes, Bogotá, Colombia*

The physical origin of dark energy remains one of the most profound open questions in modern physics. Although cosmological observations tightly constrain the equation of state parameter  $w$ , this information alone does not reveal the underlying microphysics, as many distinct theoretical models can reproduce the same expansion history. A key discriminator among these models is the sound speed of dark energy perturbations, yet this quantity remains largely unconstrained by current astrophysical observations. In this work, we propose a fundamentally new approach: using collider measurements of beyond-the-Standard-Model (BSM) mediator resonances as a probe of dark energy microphysics. We construct a unified effective-field-theory framework in which a dynamical dark energy scalar is coupled, through symmetry-motivated derivative interactions, to a pseudoscalar mediator in the 2HDM+ $a$  model. These interactions naturally induce invisible decays and modify the propagation of the BSM mediator in a dark energy background, leading to measurable distortions of resonance properties at colliders such as the LHC. We show that the decay widths, branching ratios, and kinematic structure of the mediator resonance become sensitive to the propagation properties of dark energy fluctuations, in particular the sound speed. As a result, collider observables provide a direct and complementary handle on dark energy microphysics, with the potential to distinguish between models that are otherwise indistinguishable through cosmology alone. Our results establish a new paradigm in which high-energy collider experiments can probe the physics of cosmic acceleration, revealing a connection between the smallest and largest scales in nature and opening a novel experimental pathway to uncover the fundamental origin of dark energy.

## I. INTRODUCTION

The discovery that the expansion of the Universe is accelerating revealed the presence of a dominant component of energy density, dark energy, whose microscopic origin remains one of the deepest open questions in fundamental physics [1, 2]. Despite decades of intense theoretical and observational effort, existing probes of dark energy rely almost entirely on cosmological measurements of the background expansion history or large-scale structure, leaving its underlying microphysics largely unconstrained [3–5]. In parallel, high-energy particle colliders such as the Large Hadron Collider (LHC) provide a powerful laboratory for exploring new degrees of freedom and interactions beyond the Standard Model (SM) [6, 7]. Remarkably, these two frontiers of physics, cosmic acceleration and collider experiments, have traditionally been treated as essentially disconnected. In this work we explore the possibility that they may instead be directly linked: if dark energy arises from a dynamical scalar field that interacts with new particles accessible at collider energies, then measurements of new mediator resonances at colliders such as the LHC could provide a novel probe of the microphysics responsible for cosmic acceleration [8–11].

Understanding the physical origin of cosmic acceleration remains one of the central challenges of modern cosmology. While the  $\Lambda$ CDM model successfully describes a wide range of observations, including the cosmic microwave background (CMB), large-scale structure, and Type Ia supernovae [12], the nature of dark energy – which dominates the energy density of the Universe at late times – remains unknown. The cosmological con-

stant interpretation of dark energy provides an excellent phenomenological fit to the data but raises profound theoretical puzzles, most notably the extreme discrepancy between the small observed vacuum energy and the particle-physics expectation [13].

This tension has motivated a large number of alternative scenarios ranging from modified gravity theories to dynamical scalar-field models and quantum-gravitational explanations of vacuum energy [14–17]. Many of these alternatives describe dark energy as a dynamical scalar field  $\phi$  whose dynamics are governed by a nontrivial kinetic structure. A broad and widely used description is provided by k-essence models, which we treat throughout as an effective field theory (EFT) for a shift-symmetric scalar, valid below a cutoff energy scale  $\Lambda$  [18, 19].

In such theories, the Lagrangian function  $P$  controls both the background evolution and the dynamics of perturbations. While the former is captured at leading order by the background equation-of-state parameter  $w$ , defined as the ratio of pressure to energy density for a given component ( $w \equiv p/\rho$ ), vastly different microphysical models can share nearly identical background expansion histories [20–24]. As a result, measurements of  $w$  alone cannot uniquely determine the physical origin of cosmic acceleration.

The dynamics of perturbations is governed by the sound speed of dark energy  $c_s^2$ , which controls the propagation of pressure perturbations and determines whether it clusters gravitationally on cosmological scales. In canonical scalar-field models one typically finds  $c_s^2 = 1$ , implying that dark energy remains nearly homogeneous. By contrast, a wide range of non-canonical theories – including coupled dark energy models [25–29], k-essence

scenarios [30–44], and EFT extensions of gravity [19, 45–49] – naturally predict  $c_s^2 \ll 1$  and, in some cases, superluminal propagation. Measuring or constraining this quantity therefore provides a direct window into the microphysics underlying cosmic acceleration [50, 51].

Unfortunately, whereas  $w$  is constrained at the percent level by current cosmological probes [52],  $c_s^2$  remains only weakly bounded. Existing probes primarily rely on integrated cosmological effects such as the late-time Integrated Sachs–Wolfe effect and correlations with large-scale structure [53–59], which leave substantial degeneracies among different dark energy models. Therefore, developing new and independent probes of dark energy perturbations is an important goal for both cosmology and fundamental physics.

To this end, high-energy particle colliders provide a complementary window into the fundamental structure of the dark sector. The LHC has an extensive experimental program searching for physics beyond the Standard Model (BSM) [60–82], including extended Higgs sectors [83–85], dark matter mediators [86–88], and other new particles that could reveal the microscopic structure of hidden sectors. In particular, recent analyses by the CMS and ATLAS collaborations have reported statistically significant excesses in the di-top invariant mass spectrum near the di-top mass threshold [89, 90]. These features have been discussed in the literature as possibly arising from QCD effects such as toponium formation or from a new pseudoscalar resonance associated with BSM physics.

A widely used theoretical framework in BSM extensions is the Two-Higgs-Doublet Model supplemented by a pseudoscalar mediator (2HDM+ $a$ ), which can be applied to interpret such excesses [91–95]. This model extends the scalar sector in a renormalizable manner, provides a natural portal between the SM and dark matter (DM), and predicts characteristic collider signatures including  $t\bar{t}$  resonances and missing-energy final states [86, 88]. However, in essentially all existing collider studies of the 2HDM+ $a$  framework, mediator widths and branching ratios are computed purely as functions of particle-physics parameters such as Higgs mixing angles, Yukawa couplings, and dark-matter interactions [91, 92]. Cosmology enters only indirectly through relic-density considerations [96].

Conversely, most dark energy models are built using the language of gravitational or cosmological EFT, without embedding the dark energy sector into a concrete particle-physics framework relevant for collider experiments. This separation between collider physics and dark energy phenomenology leaves largely unexplored the possibility that the physics responsible for cosmic acceleration might also leave detectable signatures in laboratory experiments.

This observation motivates the central question explored in this work: *Can collider measurements of BSM mediator resonances provide a probe of dark energy microphysics?* In this paper we develop a unified EFT

framework in which the 2HDM+ $a$  model is extended by a dynamical dark energy scalar sector with derivative couplings to the pseudoscalar mediator. These couplings are not introduced ad hoc, but arise naturally from an approximate shift-symmetry  $\phi \rightarrow \phi + \text{const}$  that protects the lightness and slow evolution of the dark energy field [97, 98]. Within this framework, interactions with the mediator emerge as a consequence of the underlying structure and can manifest through energy-dependent processes at collider scales. We show that these interactions can open a new invisible decay channel  $a \rightarrow \phi\phi$  and can renormalize the mediator kinetic term in the presence of a dark energy kinetic background. Both effects modify the pseudoscalar decay widths, branching ratios, and resonance lineshape relevant for collider searches. As a consequence, collider measurements or constraints of BSM mediator properties can become sensitive to parameters that are usually associated with dark energy EFT, including the sound speed of dark energy, defined as pressure perturbations over energy density perturbations of the dark energy field. In this way, symmetry-motivated derivative interactions provide a natural bridge between dark energy microphysics and collider observables, enabling the possibility of probing the physics of cosmic acceleration at colliders.

The remainder of this paper is organized as follows. We begin by constructing the extended EFT Lagrangian and motivating each operator from cosmological EFT considerations. We then derive the kinetic normalization of the pseudoscalar mediator and the resulting rescalings of physical masses and couplings. Next, we compute the partial decay widths, first within the context of canonical quintessence and subsequently extending the calculation to the k-essence scenario, thereby introducing explicit dependence on the sound speed of dark energy. We then analyze distinct scenarios corresponding to different assumptions about the local dark energy kinetic background, followed by a discussion of the collider implications for widths, branching ratios, and kinematic observables. Building on this, we connect the same operators to cosmological perturbation theory and examine the associated theoretical consistency conditions. Finally, we conclude with a proposed program for joint collider–cosmology inference aimed at probing the microphysics of dark energy.

## II. THEORETICAL FRAMEWORK

In order to explore how collider observables may become sensitive to the microphysics of dark energy, we construct a unified effective field theory in which a collider-motivated pseudoscalar mediator sector interacts with a dynamical dark energy scalar field. Our theoretical basis lies in the 2HDM+ $a$  model, a framework widely used to interpret heavy-flavor and missing-energy signatures at the LHC [86, 88, 91, 92]. In this model, the SM Higgs sector is extended by two Higgs doublets [83], together

with an additional pseudoscalar mediator  $a$  that mixes with the CP-odd Higgs state after electroweak symmetry breaking [91]. This mixing generates a physical pseudoscalar eigenstate that can couple both to SM fermions and to dark-sector particles [92, 93].

For the collider calculations relevant to this work, we start with couplings of the physical pseudoscalar eigenstate  $a$  to top quarks and dark matter. We write its quadratic Lagrangian as

$$\mathcal{L}_{a,0} = \frac{1}{2}(\partial a)^2 - \frac{1}{2}m_a^2 a^2, \quad (1)$$

where  $m_a$  is a Lagrangian mass parameter for the mediator in the absence of interactions with the dark energy sector. The dominant pseudoscalar couplings relevant for collider phenomenology arise from interactions with top quarks and a fermionic dark matter candidate  $\chi$ , which we write as

$$\mathcal{L}_{\text{int}}^{(t,\chi)} \supset ig_t a \bar{t}\gamma^5 t + ig_\chi a \bar{\chi}\gamma^5 \chi. \quad (2)$$

This choice is partially motivated by recent ATLAS and CMS searches for resonances in the  $t\bar{t}$  invariant mass spectrum, which have reported statistically significant excesses near the  $2m_t$  threshold [89, 90]. These interactions govern the primary decay channels relevant for di-top and missing-energy searches at the LHC. We emphasize that this setup should be regarded as a benchmark scenario chosen for concreteness and experimental relevance. However, the central results of this work are not sensitive to this restriction and can be straightforwardly generalized to cases in which the pseudoscalar mediator couples more broadly to other Standard Model fermions or bosons. In a UV-complete 2HDM+ $a$  realization the coupling  $g_t$  arises from the Yukawa structure of the two-Higgs-doublet sector and the mixing between pseudoscalar states. For the purposes of the present analysis, however, we treat  $g_t$  and  $g_\chi$  as effective couplings, to be mapped onto a specific 2HDM+ $a$  benchmark at a later stage. The above sector provides a well-defined description of pseudoscalar mediator phenomenology at colliders [94]. Our goal is to extend this framework by introducing a dark energy scalar field whose dynamics will influence the mediator properties and therefore modify collider observables.

We introduce a scalar field  $\phi$  that plays the role of dark energy and describe it using the general effective-field-theory Lagrangian

$$\mathcal{L}_\phi = P(\phi, X), \quad X \equiv -\frac{1}{2}\partial_\mu\phi\partial^\mu\phi. \quad (3)$$

This formulation encompasses a broad class of scalar-field dark energy models [99–101]. Canonical quintessence corresponds to the choice  $P = X - V(\phi)$  [102, 103], while more general k-essence theories allow nonlinear functions of  $X$  that modify the kinetic structure of the field [104]. This EFT description should be viewed as the lower-energy limit of a more fundamental theory in which the

scalar field is responsible for cosmic acceleration at late times.

Within this framework the energy density and pressure associated with the scalar field, identified as  $\rho_\phi = T_{00}$  and  $p_\phi = \frac{1}{3}(T^\mu_\mu + \rho_\phi)$ , are given by

$$p_\phi = P(\phi, X), \quad \rho_\phi = 2XP_X - P, \quad (4)$$

where  $P_X \equiv \partial P/\partial X \equiv \partial_X P$ . The dynamics of perturbations around the cosmological background are governed by the sound speed

$$c_s^2 = \frac{P_X}{P_X + 2XP_{XX}}, \quad (5)$$

where  $P_{XX} \equiv \partial^2 P/\partial X^2 = \partial_X^2 P$  [99, 100].

Note that this construction admits  $c_s^2$  to deviate significantly from unity [100, 105]. This is in contrast with canonical scalar-field models, wherein one typically finds  $c_s^2 = 1$ , implying that dark energy remains nearly homogeneous on sub-horizon scales [103, 106]. When  $c_s^2 \ll 1$ , dark energy can cluster gravitationally and participate in the growth of structure [57, 107], while other scenarios may produce superluminal propagation speeds in certain regimes. Determining or constraining this quantity therefore provides a direct probe of the microphysical structure of the dark energy sector [50, 51].

To connect the dark energy sector with collider phenomenology we consider derivative interactions between the dark energy scalar  $\phi$  and the pseudoscalar mediator  $a$ . Derivative couplings are well motivated in many scalar-field theories because approximate shift symmetries suppress direct potential interactions, resulting in the leading interaction involving derivatives of the field. An exact shift symmetry ( $\phi \rightarrow \phi + \text{constant}$ ) forbids direct potential terms such as such as mass terms or polynomial potentials, since the Lagrangian cannot depend explicitly on  $\phi$  itself [97, 98].

In this context, direct potential interactions would generically introduce large mass scales or rapid evolution for the scalar field. Such interactions are typically disfavored in dark energy model building, since they can spoil the slow-roll or slowly varying behavior required for cosmic acceleration, and can lead to strong constraints from laboratory and astrophysical tests [108–110]. By contrast, derivative interactions such as  $a(\partial\phi)^2$  are compatible with approximate shift symmetry and therefore arise naturally in effective field theories of light scalar degrees of freedom. This structure is familiar from Goldstone bosons and other modes associated with spontaneously broken symmetries, where the leading interactions are derivative-suppressed [108, 111]. In the context of dark energy, similar symmetry arguments are often invoked to ensure radiative stability of the scalar sector and to protect the small mass scale associated with cosmic acceleration.

In the present work, dark energy derivative couplings occur with the physical pseudoscalar  $a$  and can thus leave imprints on collider observables depending on the

energy scale. The leading operator that directly connects the mediator to the dark energy sector is a dimension-five derivative interaction,

$$\mathcal{L}_{a\phi\phi} = \frac{C_5}{\Lambda_5} a \partial_\mu \phi \partial^\mu \phi, \quad (6)$$

where  $\Lambda_5$  represents the characteristic mass scale of the heavy degrees of freedom that generate this operator upon being integrated out, and the coefficient  $C_5$  is a dimensionless Wilson coefficient that encodes the strength of the underlying UV interactions. The ratio  $C_5/\Lambda_5$  therefore plays the role of the effective coupling controlling the interaction at low energies. This term represents a trilinear interaction in which the mediator  $a$  can emit or absorb excitations of the scalar field  $\phi$ . In practical terms this operator opens a new invisible decay channel,  $a \rightarrow \phi\phi$ , provided that excitations of  $\phi$  are stable on collider timescales.

Physically, the dimension-five interaction allows energy stored in the mediator field to be converted into propagating fluctuations of the dark energy sector. The interpretation of this interaction can be understood by analogy with other systems in physics. For example, in electromagnetism a scalar field coupled through an operator such as  $\phi F_{\mu\nu} F^{\mu\nu}$  can source or absorb electromagnetic radiation [112–114]. Similarly, in condensed-matter systems, lattice deformations can couple to phonons, allowing energy to be transferred between background strains and propagating excitations [115, 116]. In the present case, the pseudoscalar mediator interacts with background kinetic excitations of the dark energy field in an analogous manner.

A second interaction arises at dimension eight,

$$\mathcal{L}_{\text{kinmix}} = \frac{C_8}{\Lambda_8^4} (\partial\phi)^2 (\partial a)^2, \quad (7)$$

where  $\Lambda_8$ ,  $C_8$ , and the ratio  $C_8/\Lambda_8^4$  play the roles of  $\Lambda_5$ ,  $C_5$  and  $C_5/\Lambda_5$  in the dimension-five case. Unlike the previous operator, this term does not correspond directly to a decay vertex. Instead, it modifies the kinetic structure of the mediator field when the dark energy field possesses a nonzero background gradient.

In a cosmological setting the dark energy field generically evolves in time, implying that the background value of  $X$  is nonzero. In such a background the operator in Eq. (7) induces an effective rescaling of the mediator kinetic term,  $(\partial a)^2 \rightarrow \frac{(\partial a)^2}{Z_a}$ , where the parameter  $Z_a$  depends on the background value of  $(\partial\phi)^2$ . This effect alters the normalization, propagation, and dispersion properties of the pseudoscalar field. Conceptually, this operator can be interpreted in a similar vein to the propagation of particles in a medium. For example, photons traveling through an electron plasma acquire an effective dispersion relation because the background plasma modifies their kinetic response [117, 118]. Similarly, phonons in condensed-matter systems propagate differently depending on the background properties of the lattice [115, 116].

In the present case, the cosmological dark energy background acts as a dynamical medium that modifies the effective kinetic properties of the pseudoscalar mediator.

From a collider perspective, this interaction implies that the wavefunction normalization of the mediator can depend on the dark energy background. Consequently, production rates, decay widths, and kinematic distributions of the mediator may become sensitive to parameters associated with the dark energy sector.

To ensure stability of dark energy scalar excitations, we impose a discrete  $\mathbb{Z}_2$  symmetry under which  $\phi \rightarrow -\phi$ . Under this symmetry, all operators involving an odd power of  $\phi$  fields are forbidden. In particular, linear couplings of  $\phi$  to SM fields or to other sectors are absent, preventing the decay of a single  $\phi$  quantum into lighter states. As a result,  $\phi$  excitations produced in processes such as  $a \rightarrow \phi\phi$  are stable on detector timescales and manifest as missing momentum at colliders. Note that this  $\mathbb{Z}_2$  symmetry does not prevent a time-dependent background configuration  $\bar{\phi}(t)$ , which continues to evolve according to  $P(\phi, X)$  and can drive cosmic acceleration.

The stability of the dark matter candidate  $\chi$  is, in general, an independent assumption of the 2HDM+ $a$  framework and may arise from a separate symmetry, often another  $\mathbb{Z}_2$  under which  $\chi$  is odd. In the setup considered here,  $\chi$  is taken to be stable and thus it contributes to missing-energy signatures, but its stabilization need not be tied to the  $\phi$  sector. Nevertheless, if desired, one could embed both  $\phi$  and  $\chi$  within a common discrete symmetry structure, leading to a unified origin of stability for invisible final states.

In any case, collecting the relevant terms, the effective Lagrangian governing the interactions of the mediator and the dark energy sector is

$$\begin{aligned} \mathcal{L} = & \frac{1}{2}(\partial a)^2 - \frac{1}{2}m_a^2 a^2 + ig_t a \bar{t}\gamma^5 t + ig_\chi a \bar{\chi}\gamma^5 \chi \\ & + P(\phi, X) + \frac{C_5}{\Lambda_5} a(\partial\phi)^2 + \frac{C_8}{\Lambda_8^4} (\partial\phi)^2 (\partial a)^2, \quad (8) \end{aligned}$$

providing a minimal framework in which collider observables associated with the pseudoscalar mediator can become sensitive to the kinetic structure of the dark energy sector.

### III. MEDIATOR KINETIC NORMALIZATION AND PHYSICAL PARAMETERS

Unlike the dimension-5 interaction (6), that opens a new decay channel, the dimension-8 operator (7) modifies the kinetic structure of the mediator in the presence of a nontrivial dark energy kinetic background.

It is convenient to express the interaction in terms of the scalar quantity  $X \equiv -\frac{1}{2}\partial_\mu \phi \partial^\mu \phi$ . Using the identity  $(\partial\phi)^2 \equiv \partial_\mu \phi \partial^\mu \phi = -2X$ , the kinetic mixing operator

becomes

$$\mathcal{L}_{\text{kinmix}} = \frac{C_8}{\Lambda_8^4} (\partial\phi)^2 (\partial a)^2 = \frac{-2XC_8}{\Lambda_8^4} (\partial a)^2. \quad (9)$$

We now combine this contribution with the canonical kinetic term of the mediator to obtain

$$\mathcal{L}_{a,\text{kin}} = \frac{1}{2} (\partial a)^2 - \frac{2XC_8}{\Lambda_8^4} (\partial a)^2 = \frac{1}{2} \left( 1 - \frac{4XC_8}{\Lambda_8^4} \right) (\partial a)^2. \quad (10)$$

This expression motivates the definition of a dimensionless parameter

$$Z_a \equiv 1 - 4X \frac{C_8}{\Lambda_8^4}. \quad (11)$$

The quadratic Lagrangian governing the mediator field therefore becomes

$$\mathcal{L}_{a,\text{quad}} = \frac{1}{2} Z_a (\partial a)^2 - \frac{1}{2} m_a^2 a^2. \quad (12)$$

The parameter  $Z_a$  measures how the kinetic normalization of the mediator  $a$  is modified by the background kinetic energy of the dark energy field. When  $X = 0$  the standard vacuum normalization is recovered and  $Z_a = 1$ . However, in a scenario where the dark energy field evolves in time,  $X$  acquires a nonzero expectation value and the effective normalization of the mediator field is shifted ( $Z_a \neq 1$ ). This in turn alters effective propagation properties of  $a$ .

For collider processes the relevant spacetime region is microscopic compared to cosmological length and time scales. We therefore adopt the standard EFT assumption that the background value of  $X$  is approximately constant over the spacetime region probed by a collider event. Under this separation-of-scales assumption,  $Z_a$  can be treated as a constant parameter in the calculation of mediator production and decay.

The kinetic term in Eq. (12) is not canonically normalized when  $Z_a \neq 1$ . To obtain the physical propagating field we introduce a canonically normalized field  $a_c$  defined by  $a_c \equiv \sqrt{Z_a} a$ , or equivalently,  $a = a_c / \sqrt{Z_a}$ . Since  $Z_a$  is constant, derivatives act only on the field itself:

$$\partial_\mu a = \partial_\mu \left( \frac{a_c}{\sqrt{Z_a}} \right) = \frac{1}{\sqrt{Z_a}} \partial_\mu a_c. \quad (13)$$

Substituting this relation into Eq. (12) yields

$$\begin{aligned} \mathcal{L}_{a,\text{quad}} &= \frac{1}{2} Z_a \left( \frac{1}{Z_a} (\partial a_c)^2 \right) - \frac{1}{2} m_a^2 \left( \frac{a_c}{\sqrt{Z_a}} \right)^2 \\ &= \frac{1}{2} (\partial a_c)^2 - \frac{1}{2} \frac{m_a^2}{Z_a} a_c^2. \end{aligned} \quad (14)$$

We therefore identify the physical mediator mass as

$$m_{a,\text{phys}} = \frac{m_a}{\sqrt{Z_a}}, \quad (15)$$

which demonstrates that the dark energy kinetic background induces a shift in the physical mass of the mediator. From a collider perspective this effect corresponds to a background-dependent normalization of the mediator mass.

We note that the kinetic term of a healthy propagating scalar field must have the correct sign in order to avoid ghost instabilities. This requirement implies  $Z_a > 0$ , which in turn requires that  $X < \Lambda_8^4 / 4C_8$  via Eq. (11). This inequality represents a consistency condition on the allowed range of the dark energy kinetic background relative to the cutoff scale of the effective theory.

An important consequence of canonical normalization is that all interactions linear in the mediator field acquire a rescaling factor. Consider for example the coupling to top quarks,  $ig_t a \bar{t} \gamma^5 t$ . Expressing the interaction in terms of the canonical field  $a_c$  gives

$$ig_t a \bar{t} \gamma^5 t = ig_t \left( \frac{a_c}{\sqrt{Z_a}} \right) \bar{t} \gamma^5 t. \quad (16)$$

It is therefore convenient to define the physical coupling

$$g_{t,\text{phys}} = \frac{g_t}{\sqrt{Z_a}}. \quad (17)$$

The same rescaling applies to the dark-matter coupling,

$$g_{\chi,\text{phys}} = \frac{g_\chi}{\sqrt{Z_a}}. \quad (18)$$

The derivative interaction with the dark energy field transforms in an analogous way:

$$\frac{C_5}{\Lambda_5} a (\partial\phi)^2 = \frac{C_5}{\Lambda_5} \left( \frac{a_c}{\sqrt{Z_a}} \right) (\partial\phi)^2. \quad (19)$$

Defining the physical coefficient

$$C_{5,\text{phys}} = \frac{C_5}{\sqrt{Z_a}}, \quad (20)$$

the interaction becomes

$$\mathcal{L}_{a\phi\phi} = \frac{C_{5,\text{phys}}}{\Lambda_5} a_c (\partial\phi)^2. \quad (21)$$

These results demonstrate that the kinetic mixing operator produces correlated shifts in the BSM mediator mass and its interaction strengths. Consequently, collider observables such as production cross sections, decay widths, and resonance lineshapes can become sensitive to the dark energy kinetic background encoded in the parameter  $Z_a$ .

#### IV. MEDIATOR PARTIAL WIDTHS WITH DERIVATIVE DARK ENERGY COUPLINGS

In this section we derive the mediator partial widths under a set of simplifying but well-defined assumptions

that closely parallel standard calculations in particle physics. We take the dark energy sector to be in the *canonical quintessence* limit,  $P(\phi, X) = X - V(\phi)$ , for which the field  $\phi$  is canonically normalized and Lorentz invariance remains manifest at the level of fluctuations. Expanding around a background configuration and keeping the quadratic terms for excitations, one obtains the standard relativistic scalar form

$$\mathcal{L}_{\phi,0} \supset \frac{1}{2}(\partial\phi)^2 - \frac{1}{2}m_\phi^2\phi^2, \quad (22)$$

where  $m_\phi^2 \equiv V_{\phi\phi}$  evaluated on the background. Under these assumptions, excitations of  $\phi$  propagate with the Lorentz-invariant dispersion relation  $\omega^2 = \mathbf{k}^2 + m_\phi^2$ , and the field  $\phi$  creates properly normalized asymptotic one-particle states. As a result, decay widths can be computed using the familiar two-body phase-space measure and traditional S-matrix expressions, exactly as one would for decays into ordinary scalar particles.

Conceptually, this setup corresponds to the intuitive picture in which the mediator decays into two freely propagating particles whose energy, momentum, and normalization follow the same rules as those of standard relativistic quanta. The calculation performed here therefore serves as a transparent baseline: it isolates the role of the derivative cubic interaction and allows one to track explicitly how the mediator mass, the coupling scale  $\Lambda_5$ , and the kinetic normalization parameter  $Z_a$  enter the decay rate. These assumptions do not capture the most general behavior expected of a dynamical dark energy sector. In particular, for a generic  $P(\phi, X)$  theory the fluctuations of  $\phi$  need not be canonically normalized, nor do they necessarily propagate at the speed of light. In later sections we relax these assumptions and perform a more general calculation in which the physical decay width is expressed in terms of canonically normalized perturbations and a nontrivial dispersion relation characterized by the dark energy sound speed  $c_s^2$ .

We compute the partial widths relevant for collider top and invisible searches,  $a \rightarrow t\bar{t}$ ,  $a \rightarrow \chi\bar{\chi}$ ,  $a \rightarrow \phi\phi$ , working throughout with the canonically normalized mediator field  $a_c$  and expressing results in terms of the original parameters ( $m_a, g_t, g_\chi, C_5/\Lambda_5, C_8/\Lambda_8, X$ ) via the kinetic normalization  $Z_a$  introduced in the previous section. The physical mediator mass will be simply denoted by  $m$ , such that  $m \equiv m_{a,\text{phys}} = \frac{m_a}{\sqrt{Z_a}}$ .

When  $Z_a \simeq 1$ , the mediator is essentially canonically normalized at collider scales and the dominant effect of the dark energy sector is the opening of the new invisible channel through the dimension-5 operator. This would be the case in the cosmological-background-only expectation, since  $X$  (set by the homogeneous dark energy kinetic density) would be extraordinarily small in collider units and thus  $4XC_8/\Lambda_8^4 \ll 1$  for any  $\Lambda_8$  near or above the electroweak scale. Meanwhile, when  $Z_a$  differs appreciably from unity, the mediator wavefunction normalization, physical mass, and all linear couplings are simultaneously rescaled, leading to correlated shifts across

visible and invisible channels. This scenario can be interpreted as a parameterization of nontrivial local kinetic backgrounds, for example in environments where gradients are enhanced or where the EFT admits localized configurations. In such cases, the term  $4XC_8/\Lambda_8^4$  need not be much less than 1, and thus we may have  $0 < Z_a < 1$ . Physically, the dimension-8 operator makes the mediator propagate in an effective medium set by the local value of  $(\partial\phi)^2$ .

### A. Decay $a \rightarrow \phi\phi$ from the derivative cubic

We begin by computing the partial decay width of the pseudoscalar mediator into two dark energy quanta,  $a_c \rightarrow \phi\phi$ , arising from the derivative interaction introduced in the previous section. In the canonical quintessence limit, the field  $\phi$  behaves as a standard relativistic scalar, and the calculation can be performed using familiar S-matrix techniques. From Eq. (21), the interaction relevant for this decay is

$$\mathcal{L} \supset \frac{C_5}{\Lambda_5\sqrt{Z_a}} a_c \partial_\mu \phi \partial^\mu \phi. \quad (23)$$

This operator describes a trilinear interaction in which the mediator couples to the local kinetic energy density of the  $\phi$  field. As a result, the decay amplitude is proportional to the momenta carried by the outgoing particles.

To calculate the decay amplitude, we consider the decay process

$$a_c(p) \rightarrow \phi(p_1) \phi(p_2), \quad p = p_1 + p_2, \quad (24)$$

where  $p$  is the four-momentum of the mediator and  $p_1, p_2$  are the momenta of the final-state particles. In momentum space, each derivative acting on an external  $\phi$  field contributes a factor of  $ip_\mu$ . Applying this rule to Eq. (23), the tree-level squared matrix element becomes

$$|\mathcal{M}|^2 = \left( \frac{c}{\Lambda\sqrt{Z_a}} \right)^2 (p_1 \cdot p_2)^2, \quad (25)$$

from which we can see that the interaction is momentum-suppressed. To proceed with the evaluation of kinematic invariants, we express the Lorentz-invariant product  $p_1 \cdot p_2$  in terms of physical masses. Using the identity

$$p^2 = (p_1 + p_2)^2 = p_1^2 + p_2^2 + 2p_1 \cdot p_2, \quad (26)$$

and imposing the on-shell conditions  $p^2 = m^2$  and  $p_1^2 = p_2^2 = m_\phi^2$ , we obtain

$$m^2 = 2m_\phi^2 + 2p_1 \cdot p_2, \quad (27)$$

which can be rearranged to give

$$p_1 \cdot p_2 = \frac{m^2 - 2m_\phi^2}{2}. \quad (28)$$

Substituting this expression into Eq. (25), the squared amplitude becomes

$$|\mathcal{M}|^2 = \frac{C_5^2}{\Lambda_5^2 Z_a} \frac{(m^2 - 2m_\phi^2)^2}{4}. \quad (29)$$

This form makes the dependence on both the mediator mass and the dark energy scalar mass explicit.

The partial decay width is then computed using the standard two-body phase-space formula,

$$\Gamma = \frac{1}{2m} \frac{1}{2!} \int d\Phi_2 |\mathcal{M}|^2, \quad (30)$$

where the factor of  $1/2!$  accounts for the identical  $\phi$  particles in the final state. The integrated two-body phase space is given by

$$\int d\Phi_2 = \frac{1}{8\pi} \beta_\phi, \quad \beta_\phi \equiv \sqrt{1 - \frac{4m_\phi^2}{m^2}}, \quad (31)$$

where  $\beta_\phi$  represents the velocity of the final-state particles in the rest frame of the decaying mediator. Substituting Eq. (31) into Eq. (30), we obtain

$$\Gamma(a_c \rightarrow \phi\phi) = \frac{|\mathcal{M}|^2}{32\pi m} \beta_\phi, \quad (32)$$

and finally, inserting Eq. (29) yields

$$\Gamma(a_c \rightarrow \phi\phi) = \frac{C_5^2}{128\pi} \frac{(m^2 - 2m_\phi^2)^2}{\Lambda_5^2 Z_a m} \sqrt{1 - \frac{4m_\phi^2}{m^2}}. \quad (33)$$

It is useful to express the result in terms of the original Lagrangian mass parameter  $m_a$  and the kinetic normalization  $Z_a$ . Using the relation  $m^2 = \frac{m_a^2}{Z_a}$ , we obtain

$$\begin{aligned} \Gamma(a \rightarrow \phi\phi) &= \frac{C_5^2}{128\pi} \frac{(m_a^2 - 2Z_a m_\phi^2)^2}{\Lambda_5^2 m_a} \\ &\times Z_a^{-5/2} \sqrt{1 - \frac{4Z_a m_\phi^2}{m_a^2}}. \end{aligned} \quad (34)$$

This expression highlights the nontrivial scaling with  $Z_a$ , which arises from the combined effects of field normalization, coupling rescaling, and phase space.

In many phenomenologically relevant scenarios, the dark energy scalar is extremely light compared to collider scales,  $m_\phi \ll m_a$  [101–103]. In this limit, the phase-space suppression becomes negligible and the expression simplifies considerably:

$$\Gamma(a \rightarrow \phi\phi) \xrightarrow{m_\phi \rightarrow 0} \frac{C_5^2}{128\pi} \frac{m_a^3}{\Lambda_5^2} Z_a^{-5/2}. \quad (35)$$

We see explicitly that the invisible decay width scales as  $m_a^3$  and is strongly enhanced for small  $Z_a$ , reflecting the sensitivity of the decay to the underlying dark energy background through kinetic mixing.

## B. Decay $a \rightarrow t\bar{t}$ and $a \rightarrow \chi\bar{\chi}$

We now summarize the partial decay widths of the pseudoscalar mediator into fermionic final states, focusing on the top-quark channel and the dark matter channel. These decay modes are standard in the literature for pseudoscalar mediators and serve as the primary visible and invisible benchmarks against which the new dark energy channel will be compared [87, 91, 92, 94].

In terms of the canonically normalized mediator field  $a_c$ , the relevant interaction Lagrangian is given by

$$\mathcal{L} \supset ig_t^{(\text{phys})} a_c \bar{t} \gamma^5 t + ig_\chi^{(\text{phys})} a_c \bar{\chi} \gamma^5 \chi, \quad g_{t,\chi}^{(\text{phys})} = \frac{g_{t,\chi}}{\sqrt{Z_a}}. \quad (36)$$

As discussed previously, the factor of  $Z_a^{-1/2}$  arises from the canonical normalization of the mediator field, and implies that all fermionic couplings inherit a dependence on the dark energy kinetic background.

The decay width of a pseudoscalar particle into a Dirac fermion pair  $f\bar{f}$  is well known and can be written in the compact form

$$\Gamma(a_c \rightarrow f\bar{f}) = N_c \frac{(g_f^{(\text{phys})})^2}{8\pi} m \sqrt{1 - \frac{4m_f^2}{m^2}}, \quad (37)$$

where  $N_c$  is the number of colors of the fermion,  $m$  is the physical mass of the mediator, and the square-root factor encodes the usual two-body phase-space suppression near threshold.

Applying this general result to the top-quark final state, and recalling that  $N_c = 3$  for quarks, we obtain

$$\Gamma(a_c \rightarrow t\bar{t}) = 3 \frac{(g_t^{(\text{phys})})^2}{8\pi} m \sqrt{1 - \frac{4m_t^2}{m^2}}. \quad (38)$$

Substituting the relations  $g_t^{(\text{phys})} = g_t/\sqrt{Z_a}$  and  $m = m_a/\sqrt{Z_a}$ , derived in the previous section, leads to the expression

$$\Gamma(a \rightarrow t\bar{t}) = 3 \frac{g_t^2 m_a}{8\pi} Z_a^{-3/2} \sqrt{1 - \frac{4Z_a m_t^2}{m_a^2}}, \quad (39)$$

which makes explicit how the kinetic normalization parameter  $Z_a$  modifies both the overall normalization and the kinematic threshold of the decay.

An entirely analogous calculation applies to the dark matter channel. Assuming a Dirac fermion  $\chi$  with pseudoscalar coupling  $g_\chi$ , the decay width is given by

$$\Gamma(a_c \rightarrow \chi\bar{\chi}) = \frac{(g_\chi^{(\text{phys})})^2}{8\pi} m \sqrt{1 - \frac{4m_\chi^2}{m^2}}. \quad (40)$$

Expressing this in terms of the original Lagrangian parameters yields

$$\Gamma(a \rightarrow \chi\bar{\chi}) = \frac{g_\chi^2 m_a}{8\pi} Z_a^{-3/2} \sqrt{1 - \frac{4Z_a m_\chi^2}{m_a^2}}. \quad (41)$$

For completeness, we note that if the dark matter particle is Majorana rather than Dirac, the decay width in Eq. (41) is reduced by a factor of 1/2 due to identical-particle statistics. We emphasize that the presence of the dark energy sector introduces a nontrivial and correlated dependence on  $Z_a$ .

### C. Total width, branching ratios, and the role of $Z_a$

Having derived the individual partial widths, we now combine these results to obtain the total decay width and branching fractions of the pseudoscalar mediator. These quantities are directly related to collider observables, such as resonance lineshapes, signal rates, and missing-energy signatures, and therefore provide the primary link between the underlying Lagrangian and experimental measurements.

In the dominant-channels approximation emphasized in this work, the total decay width can be written as

$$\Gamma_{\text{tot}} \simeq \Gamma(a \rightarrow t\bar{t}) + \Gamma(a \rightarrow \chi\bar{\chi}) + \Gamma(a \rightarrow \phi\phi). \quad (42)$$

This expression captures the leading visible and invisible decay modes relevant for LHC searches in the parameter space of interest. From the total width, the branching fraction into a given final state  $i$  is defined in the usual way as

$$\text{BR}(a \rightarrow i) = \frac{\Gamma(a \rightarrow i)}{\Gamma_{\text{tot}}}, \quad i \in \{t\bar{t}, \chi\bar{\chi}, \phi\phi\}. \quad (43)$$

It is these branching ratios, together with the total width, that determine the relative strength of different collider signatures, including di-top resonances and missing-energy final states.

### D. Role of $Z_a$ and physical interpretation

A central result of this framework is that all partial widths inherit a dependence on the kinetic-normalization parameter  $Z_a$ , which encodes the effect of the dark energy background on the mediator sector. As discussed previously,  $Z_a$  modifies both the physical mass and the effective couplings of the mediator, and therefore enters all decay rates in a correlated manner.

In the regime where  $Z_a \simeq 1$ , corresponding to the expectation that the LHC probes only the homogeneous cosmological dark energy background, the mediator is effectively canonically normalized. In this limit, the kinematic thresholds and visible decay rates are close to their standard values, and the primary new effect arises from the additional invisible decay channel  $a \rightarrow \phi\phi$ . Even in this conservative scenario, the presence of this channel can significantly alter collider observables by increasing the total width and suppressing the visible branching fractions. In particular, a nonzero  $\Gamma(a \rightarrow \phi\phi)$  leads

to a reduction in  $\text{BR}(a \rightarrow t\bar{t})$  and a corresponding enhancement of missing-energy signatures, providing a direct handle on the derivative coupling.

When  $Z_a \neq 1$ , the mediator propagates in an effective medium determined by the local kinetic background of the dark energy field. The physical mass is shifted according to  $m = m_a/\sqrt{Z_a}$ , which modifies the available phase space for all decay channels. At the same time, the effective couplings are rescaled, leading to a nontrivial dependence of the widths on  $Z_a$ .

Importantly, the different decay channels scale differently with  $Z_a$ :

$$\Gamma(a \rightarrow \phi\phi) \propto Z_a^{-5/2}, \quad \Gamma(a \rightarrow t\bar{t}, \chi\bar{\chi}) \propto Z_a^{-3/2}. \quad (44)$$

This difference in scaling implies that even moderate deviations from  $Z_a = 1$  can induce sizable and correlated changes in the branching ratios. In particular, the dark energy channel is more sensitive to the case of  $Z_a < 1$  than the fermionic channels, making it a powerful probe of dark energy effects.

### E. Implications for collider searches

The phenomenological impact of these effects depends sensitively on the mediator mass. In the region  $m_a \simeq 350\text{--}400$  GeV, the decay  $a \rightarrow t\bar{t}$  lies close to threshold, and the phase-space factor  $\sqrt{1 - (4Z_a m_t^2/m_a^2)}$  plays a crucial role. In this regime, even small shifts in  $Z_a$  can lead to large changes in the visible width, since the decay is highly sensitive to the available phase space. As a result, the interplay between the threshold suppression and the additional invisible channel can significantly distort the di-top invariant-mass distribution, providing a particularly sensitive probe of the underlying dynamics.

Away from the threshold region, for mediator masses well above  $2m_t$ , the phase-space suppression becomes negligible and the fermionic widths scale approximately linearly with  $m_a$ . In this regime, the relative importance of the dark energy channel is controlled primarily by the ratio

$$\frac{\Gamma(a \rightarrow \phi\phi)}{\Gamma(a \rightarrow t\bar{t})} \sim \frac{C_5^2 m_a^2}{\Lambda_5^2 g_t^2} Z_a^{-1}. \quad (45)$$

This scaling shows that at higher masses, the invisible decay mode can become increasingly important, particularly for moderately large values of the derivative coupling  $C_5/\Lambda_5$ .

As a consequence, even in the absence of a near-threshold enhancement, the dark energy channel can lead to observable deviations in both the total width and the branching ratios. These effects would manifest as a broadening of the resonance and a redistribution of signal strength between visible and invisible final states, which could be probed at colliders such as the LHC through a combination of di-top searches and missing-energy analyses. Importantly, these effects are not restricted to a

narrow mass window, but persist across a wide range of mediator masses. This implies that the framework developed in this work can be tested not only in the context of current di-top excesses, but also in future searches for heavier BSM pseudoscalar resonances.

The results presented here demonstrate that the parameter  $Z_a$  provides a direct bridge between dark energy physics and collider observables. In the next section, we move beyond the canonical quintessence limit and consider a more general  $P(\phi, X)$  theory. This allows us to express the decay width in terms of the sound speed of dark energy  $c_s^2$ , thereby making explicit the connection between collider measurements and the microphysics of cosmic acceleration.

## V. COLLIDER DEPENDENCE ON THE DARK ENERGY SOUND SPEED

In the preceding sections, we constructed an EFT extension of the 2HDM+ $a$  framework in which a dynamical dark energy scalar  $\phi$  couples derivatively to the pseudoscalar mediator  $a$ . Two operators were shown to play distinct and complementary roles: the dimension-5 interaction  $a(\partial\phi)^2/\Lambda_5$  opens the invisible decay channel  $a \rightarrow \phi\phi$ , while the dimension-8 kinetic-mixing operator  $(\partial\phi)^2(\partial a)^2/\Lambda_8^4$  renormalizes the mediator kinetic term in the presence of a nonzero dark energy kinetic background  $X \equiv -\frac{1}{2}(\partial\phi)^2$ . Up to this point, the analysis has been performed under the simplifying assumption that the dark energy sector behaves as a canonically normalized relativistic scalar.

We now move beyond this canonical quintessence limit and present a central result of this work: collider observables, including the mediator width, branching fractions, and resonance kinematics, can acquire a direct and calculable dependence on the *sound speed of dark energy*,  $c_s^2$ , in more general settings. The origin of this dependence is subtle but physically transparent. *While the interaction Lagrangian is written in terms of the field  $\phi$ , the particles produced at colliders correspond to fluctuations around a cosmological background*, and these fluctuations are governed by a nontrivial quadratic action in a general  $P(\phi, X)$  theory. As a result, their normalization and dispersion relation differ from those of canonical relativistic particles, and this difference feeds directly into both the decay amplitude and the available phase space.

To make this connection explicit, we adopt a well-motivated k-essence framework in which the late-time dynamics are characterized by a constant normalization  $\kappa \equiv P_X$ . This assumption is well motivated, since cosmological observations indicate that dark energy closely approximates a slowly evolving component at late times [52], implying that the background field evolution is strongly suppressed [101, 103]. In this regime, higher-order time dependence in  $P(\phi, X)$  contributes only subleading corrections to the background expansion, while the leading phenomenological effects relevant for perturbations, such

as the sound speed and normalization of kinetic fluctuations, are captured by derivatives of  $P$  evaluated on the background [100, 105]. As a result, treating  $\kappa$  as constant provides a model-independent parametrization of late-time dark energy that isolates the microphysical properties controlling perturbations without loss of generality for the collider–cosmology connection explored here. In this limit, the sound speed can be written as

$$\Sigma \equiv P_X + 2\bar{X}P_{XX}, \quad c_s^2 = \frac{P_X}{\Sigma} = \frac{\kappa}{\Sigma}, \quad (46)$$

where  $\bar{X} = \frac{1}{2}\dot{\phi}^2$  is the background kinetic energy. This relation can be inverted to express the normalization of fluctuations as

$$\Sigma = \frac{\kappa}{c_s^2}, \quad (47)$$

which makes clear that the sound speed controls the relative weight of temporal and spatial derivatives in the quadratic action.

It is useful to provide an estimate of the expected magnitude and range of  $\kappa$ . By definition,  $\kappa = P_X$  evaluated on the cosmological background controls the normalization of the kinetic term for fluctuations and therefore sets the overall scale relating field gradients to physical energy density. In canonical quintessence models, where  $P(\phi, X) = X - V(\phi)$ , one has  $P_X = 1$ , corresponding to  $\kappa = 1$  in natural units. More generally, in k-essence theories  $\kappa$  can deviate from unity, but theoretical consistency and observational constraints impose important bounds on its allowed values.

First, the absence of ghost instabilities requires  $P_X > 0$ , implying  $\kappa > 0$ . Second, the requirement that the dark energy equation of state remains close to  $w \simeq -1$  at late times implies that the kinetic contribution to the energy density is subdominant,  $XP_X \ll V(\phi)$ , but does not directly fix the normalization  $\kappa$  itself. Instead,  $\kappa$  determines how fluctuations are canonically normalized relative to the background energy density.

From an effective field theory perspective, it is natural to expect  $\kappa$  to be of order unity in the absence of additional symmetries or strong-coupling effects, since it corresponds to the leading coefficient in a derivative expansion. Values  $\kappa \ll 1$  would indicate a suppressed kinetic term and can lead to strong-coupling behavior for fluctuations, while  $\kappa \gg 1$  corresponds to an enhanced kinetic normalization, which can arise in certain non-canonical or screening scenarios.

In the present work, we therefore treat  $\kappa$  as a positive parameter of order unity,  $\kappa \sim \mathcal{O}(1)$ , while allowing for deviations to capture non-canonical dark energy dynamics. Importantly, as will be shown in the remainder of this manuscript, decay widths depend on  $\kappa$  primarily through inverse powers such as  $\kappa^{-1}$  and  $\kappa^{-2}$ , so that even  $\mathcal{O}(1)$  variations can lead to parametrically distinct phenomenological effects.

At the level of the cosmological background, we can use the equation  $\rho_\phi + p_\phi = 2XP_X$  to relate the kinetic

density  $X$  to the dark energy equation of state  $w$ . This yields

$$X = \frac{\rho_\phi(1+w)}{2\kappa}. \quad (48)$$

This expression highlights an important separation of physical roles: the parameter  $w$  determines the size of the background kinetic density and therefore controls the kinetic-mixing effect encoded in  $Z_a$ , while the sound speed  $c_s^2$  controls the dynamics of fluctuations and thus governs the production and propagation of dark energy quanta at colliders.

Substituting this result into the expression for the kinetic normalization parameter gives

$$Z_a = 1 - \frac{4XC_8}{\Lambda_8^4} = 1 - \frac{2C_8\rho_\phi(1+w)}{\kappa\Lambda_8^4}, \quad (49)$$

demonstrating that  $Z_a$  is sensitive to the background evolution but, in this framework, does not depend explicitly on  $c_s^2$ . The sound-speed dependence instead enters through the properties of the produced final-state particles.

We now explicitly derive the dependence of collider observables on the sound speed by taking the standard approach of decomposing the scalar field into a cosmological background and a fluctuation,

$$\phi = \bar{\phi}(t) + \delta\phi, \quad (50)$$

where  $\bar{\phi}(t)$  describes the homogeneous time-dependent background and  $\delta\phi$  represents small perturbations around this background, which correspond to the physical quanta that can be produced at colliders.

The dynamics of these fluctuations are obtained by expanding the Lagrangian  $P(\phi, X)$  about the background configuration  $\text{bg} \equiv (\bar{\phi}(t), \bar{X})$  [100, 104]. We can then write

$$P(\phi, X) = P(\bar{\phi}, \bar{X}) + \left. \frac{\partial P}{\partial \phi} \right|_{\text{bg}} \delta\phi + \left. \frac{\partial P}{\partial X} \right|_{\text{bg}} \delta X + \frac{1}{2} \left. \frac{\partial^2 P}{\partial X^2} \right|_{\text{bg}} (\delta X)^2 + \dots, \quad (51)$$

where  $\delta X = \dot{\bar{\phi}} \partial_0 \delta\phi$  and  $\delta X^2 = \frac{1}{2}(\partial_0 \delta\phi)^2 - \frac{1}{2}(\nabla \delta\phi)^2$  contain terms linear and quadratic in  $\delta\phi$ .

The zeroth-order term  $P(\bar{\phi}, \bar{X})$  contributes only to the background energy density and pressure, and therefore does not affect the dynamics of fluctuations. The linear terms vanish upon using the background equations of motion, which ensure that  $\bar{\phi}(t)$  extremizes the action [119, 120]. As a result, the leading contribution governing the propagation of fluctuations arises from the quadratic terms in the expansion [100].

Keeping only terms quadratic in  $\delta\phi$  and its derivatives, one obtains the effective k-essence quadratic Lagrangian for the fluctuations [100]. In the preferred cosmological frame, this takes the schematic form

$$\mathcal{L}^{(2)} \supset \frac{1}{2} \Sigma (\partial_0 \delta\phi)^2 - \frac{1}{2} \kappa (\nabla \delta\phi)^2, \quad (52)$$

where  $\Sigma$  and  $\kappa$  are evaluated on the background.

We see that time and spatial derivatives enter with different coefficients, reflecting the fact that the time-dependent background  $\bar{\phi}(t)$  spontaneously breaks Lorentz invariance by selecting a preferred rest frame. The equation of motion derived from this quadratic action then leads to the dispersion relation

$$\omega^2 = c_s^2 k^2, \quad (53)$$

where the sound speed is given by Eq. (46). Thus, the sound speed emerges as the ratio of the coefficients of spatial and temporal kinetic terms, and directly controls the propagation of the dark energy fluctuations that appear as final-state particles in collider processes.

In order to compute decay rates using standard S-matrix methods, it is convenient to introduce a canonically normalized field,

$$\phi_c \equiv \sqrt{\Sigma} \delta\phi = \sqrt{\frac{\kappa}{c_s^2}} \delta\phi, \quad (54)$$

so that the fluctuations have a standard kinetic term in time. This redefinition implies that derivatives of  $\delta\phi$  are related to those of  $\phi_c$  by

$$(\partial \delta\phi)^2 = \frac{c_s^2}{\kappa} (\partial \phi_c)^2, \quad (55)$$

which will play a crucial role in determining the effective interaction strength.

Substituting this relation into the derivative cubic interaction and expressing the mediator in terms of its canonically normalized field  $a_c$ , we obtain an effective interaction of the form

$$\mathcal{L} \supset g a_c (\partial \phi_c)^2, \quad g = \frac{C_5}{\Lambda_5} \frac{c_s^2}{\kappa} \frac{1}{\sqrt{Z_a}}. \quad (56)$$

Thus, we find that the sound speed enters the interaction strength through the canonical normalization of the dark energy fluctuations.

We now compute the decay amplitude for  $a_c \rightarrow \phi_c \phi_c$ . In momentum space, the derivative structure in Eq. 56 implies that the matrix element is proportional to the Lorentz-invariant product of the outgoing momenta, such that  $\mathcal{M} = ig(p_1 \cdot p_2)$ , where  $p_1$  and  $p_2$  are the momenta of the final-state particles  $\phi_c$  and  $p_1 \cdot p_2 = -\omega_1 \omega_2 + \mathbf{p}_1 \cdot \mathbf{p}_2$ . In the rest frame of the mediator  $a_c$ , energy conservation together with the modified dispersion relation  $\omega = c_s |\mathbf{k}|$  fixes the kinematics of the final state. In particular, one finds that the magnitude of the three-momentum scales as  $|\mathbf{p}| \sim m/(2c_s)$ , which differs from the case of canonical quintessence by a factor of  $1/c_s$ . Evaluating the invariant product then yields

$$p_1 \cdot p_2 = -\frac{m^2}{4} \left(1 + \frac{1}{c_s^2}\right), \quad (57)$$

and therefore the squared amplitude becomes

$$|\mathcal{M}|^2 = g^2 \frac{m^4}{16} \left(1 + \frac{1}{c_s^2}\right)^2. \quad (58)$$

The second ingredient entering the decay width is the two-body phase space, which determines the density of accessible final states. In the standard case of canonical quintessence, this quantity depends only on the masses of the particles. However, in the present setup the dispersion relation of the final-state quanta is modified, and this leads to a nontrivial dependence of the phase-space measure on the sound speed  $c_s$ . The starting point is the Lorentz-invariant phase-space element,

$$d\Phi_2 = \int \frac{d^3\mathbf{p}_1}{(2\pi)^3 2\omega_1} \frac{d^3\mathbf{p}_2}{(2\pi)^3 2\omega_2} (2\pi)^4 \delta^{(4)}(p-p_1-p_2), \quad (59)$$

where the energies  $\omega_i$  now satisfy the modified dispersion relation  $\omega_i = c_s |\mathbf{p}_i|$ . Working in the rest frame of the decaying mediator  $a_c$ , the spatial delta function enforces  $\mathbf{p}_2 = -\mathbf{p}_1$ , while the energy delta function imposes  $m = \omega_1 + \omega_2 = 2c_s |\mathbf{p}|$ , which fixes the magnitude of the three-momentum to be  $|\mathbf{p}| = \frac{m}{2c_s}$  as mentioned previously.

Relative to the standard case, this relation shows that a given energy corresponds to a larger spatial momentum when  $c_s < 1$ . This modifies both the momentum measure  $d^3\mathbf{p}$  and the Jacobian associated with the energy-conserving delta function. Performing the angular integrals and evaluating the remaining delta function, one finds that the phase-space measure acquires an overall enhancement factor that depends on the sound speed. The final result can be written as

$$\int d\Phi_2 = \frac{1}{8\pi c_s^3}. \quad (60)$$

The factor of  $c_s^{-3}$  has a clear physical interpretation: for subluminal propagation ( $c_s < 1$ ), the same total energy can be distributed among final states with larger momenta, effectively increasing the density of accessible states. This enhancement plays a crucial role in amplifying the decay width into dark energy quanta and is one of the key mechanisms through which the sound speed enters collider observables. In the canonical quintessence limit  $c_s = 1$ , this expression reduces to the standard massless two-body result,

$$\int d\Phi_2 \Big|_{c_s=1} = \frac{1}{8\pi}, \quad (61)$$

so the factor  $c_s^{-3}$  directly quantifies the departure from the ordinary relativistic phase space.

Combining the amplitude and phase space, the decay width is found to be

$$\Gamma(a_c \rightarrow \phi_c \phi_c) = \frac{g^2 m^3}{512\pi} \frac{(1 + c_s^2)^2}{c_s^3}. \quad (62)$$

Substituting the expression for the effective coupling  $g$  and expressing the result in terms of the original Lagrangian parameters yields the central result

$$\Gamma(a_c \rightarrow \phi_c \phi_c) = \frac{C_5^2}{512\pi} \frac{m_a^3}{\kappa^2 \Lambda_5^2} Z_a^{-5/2} \frac{(1 + c_s^2)^2}{c_s^3}. \quad (63)$$

This expression makes explicit that the sound speed controls the invisible decay width through the factor

$$\mathcal{G}(c_s) = \frac{(1 + c_s^2)^2}{c_s^3}, \quad (64)$$

which grows rapidly for  $c_s^2 \ll 1$ . Physically, this enhancement arises from two effects acting in concert: the derivative structure of the interaction, which introduces additional momentum dependence, and the modified phase space, which increases the density of accessible final states.

The collider implications of this result are immediate. Since the invisible width enters directly into the total width  $\Gamma_{\text{tot}} \simeq \Gamma(a \rightarrow t\bar{t}) + \Gamma(a \rightarrow \chi\bar{\chi}) + \Gamma(a \rightarrow \phi\phi)$ , the sound speed controls the resonance lineshape and branching ratios. Decreasing  $c_s^2$  leads to an enhanced invisible width, which in turn broadens the resonance and suppresses visible branching fractions. These effects persist across the full mediator mass range, and are not limited to the near-threshold region.

To illustrate these features, Fig. (1) shows color maps of the normalized total width,  $\Gamma_{\text{tot}}/m_{a,\text{phys}}$ , as a function of  $c_s^2$  and  $Z_a$ . The four panels correspond to two representative mediator masses,  $m_a = 365$  and  $1000$  GeV, chosen to probe the region near the  $t\bar{t}$  production threshold and a substantially heavier resonance, respectively, and two values of  $\kappa$ , namely  $\kappa = 0.5$  and  $1$ . The remaining parameters are fixed to  $m_\chi = 100$  GeV and  $g_t = g_\chi = 0.25$ , as indicated in the figure titles. These values are typical benchmarks used in dark sector collider searches [121]. The discrete color scale, shown on the right, spans values of  $\Gamma_{\text{tot}}/m_{a,\text{phys}}$  between 0 and 1. We focus primarily on the region  $0.01 \lesssim \Gamma_{\text{tot}}/m_{a,\text{phys}} \lesssim 0.2$  since widths at the percent level are characteristic of many SM resonances and are also consistent with the narrow-width interpretation of the recently reported di-top excesses by CMS and ATLAS [89, 90]. At the same time, broader resonances are well motivated in many BSM extensions, making it important to understand how the width depends on the underlying dark energy microphysics. The resonance width also plays a central role in collider phenomenology, influencing both signal modeling and the validity of common theoretical approximations [61]. As shown in Fig. (1), the normalized width generally increases as either  $c_s^2$  or  $Z_a$  decreases. The relative importance of these parameters, however, varies across the parameter space. For  $c_s^2$  close to unity, the width is primarily controlled by  $Z_a$ , while the dependence on  $c_s^2$  becomes increasingly pronounced as one approaches the  $\Gamma_{\text{tot}}/m_{a,\text{phys}} \approx 0.1$  contour (shown in red). Below this threshold, the width grows rapidly with decreasing  $c_s^2$ , eventually reaching the perturbative unitarity limit  $\Gamma_{\text{tot}}/m_{a,\text{phys}} = 1$ . These results suggest that collider measurements of the mediator width could provide a direct probe of the dark energy sector. In particular, the width is highly sensitive to  $c_s^2$  when  $c_s^2 \ll 1$ , while retaining significant sensitivity to  $Z_a$  throughout the parameter space considered. Consequently, precision measurements of the resonance line

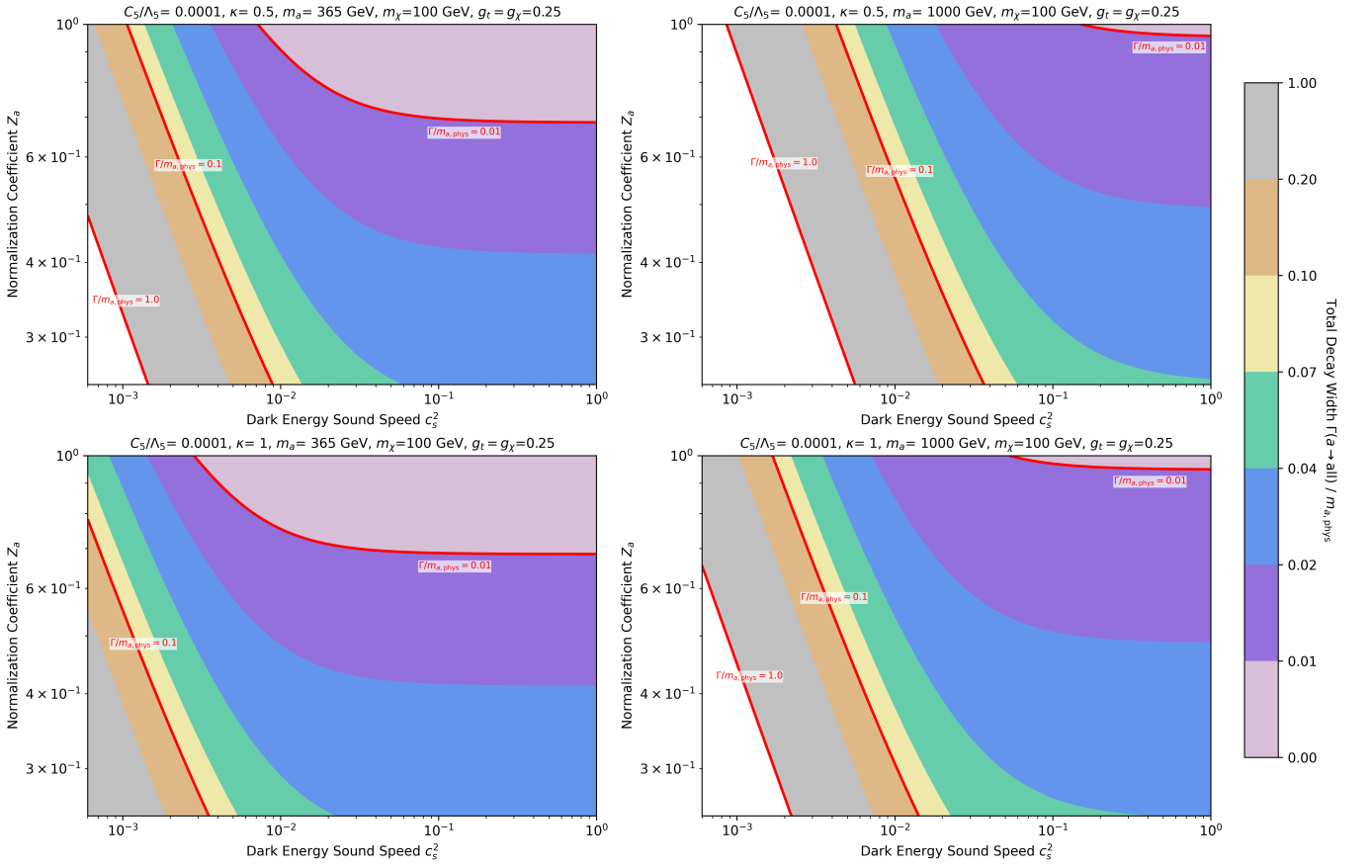


FIG. 1: Color maps of the total normalized decay width  $\Gamma_{\text{tot}}/m_{a,\text{phys}}$ , with discrete colors corresponding to different intervals between a normalized width of 0 and 1. We plot  $c_s^2$  on the horizontal axis and  $Z_a$  on the vertical axis, and vary the parameters  $m_a$  and  $\kappa$  across the four plots. Contours for  $\Gamma_{\text{tot}}/m_{a,\text{phys}} = 0.01, 0.1$ , and  $1$  are drawn in red.

shape and decay width at colliders could offer a unique window into the microphysical properties of the dark energy field  $\phi$ , complementing traditional cosmological probes.

Next, we plot the branching ratios of the visible and invisible parts of the decay versus  $c_s^2$  in Fig. (2). Here, we define

$$\text{BR}(\text{visible}) = \text{BR}(a \rightarrow t\bar{t}) = \frac{\Gamma(a \rightarrow t\bar{t})}{\Gamma_{\text{tot}}} \quad (65)$$

and

$$\begin{aligned} \text{BR}(\text{invisible}) &= \text{BR}(a \rightarrow \chi\bar{\chi}) + \text{BR}(a \rightarrow \phi\phi) \\ &= \frac{\Gamma(a \rightarrow \chi\bar{\chi}) + \Gamma(a \rightarrow \phi\phi)}{\Gamma_{\text{tot}}}. \end{aligned} \quad (66)$$

The four curves correspond to different combinations of  $(\kappa, Z_a)$ , with other parameters set to  $C_5/\Lambda_5 = 10^{-4}$ ,  $m_\chi = 100$  GeV, and  $g_t = g_\chi = 0.25$ . This plot displays that the  $a \rightarrow$  invisible channel behaves quite differently from the  $a \rightarrow$  visible channel, which is due to the derivative coupling  $\sim a(\partial\phi)^2$  in the Lagrangian term coupling  $a$  to the dark energy field  $\phi$ . We again observe that  $Z_a$  dominates the behavior for  $c_s^2 \sim 1$ . Meanwhile,

for lower sound speeds we see that  $\kappa$  significantly affects the branching ratios, with an increase in  $\kappa$  generally causing an increase in BR(visible) and a decrease in BR(invisible). For all parameter values, including the canonical case of  $(\kappa, Z_a) = (1, 1)$ , there is a clear dependency on  $c_s^2$  in both channels with high sensitivity at lower sound speeds.

Finally, we investigate the impact of dark energy microphysics on collider kinematics by studying the transverse-momentum ( $p_T$ ) distribution of the top quarks in the process  $pp \rightarrow a \rightarrow t\bar{t}$ , shown in Fig. 3. The distributions are generated using the matrix-element event generator `MadGraph5_aMC@NLO` [122], assuming proton-proton collisions at  $\sqrt{s} = 13.6$  TeV, and analyzed with `MadAnalysis5` [123]. At leading order, the top and anti-top quarks are produced back-to-back in the transverse plane and therefore share identical  $p_T$  distributions. The four histograms correspond to different choices of the dark energy parameters  $(c_s^2, Z_a)$ , as indicated in the legend. All other model parameters are fixed to the values used in the lower-left panel of Fig. 3. For the black histogram, we additionally set  $C_5/\Lambda_5 = 0$ , corresponding to a canonically normalized mediator completely decoupled from the dark energy field. It serves as a ‘‘baseline’’

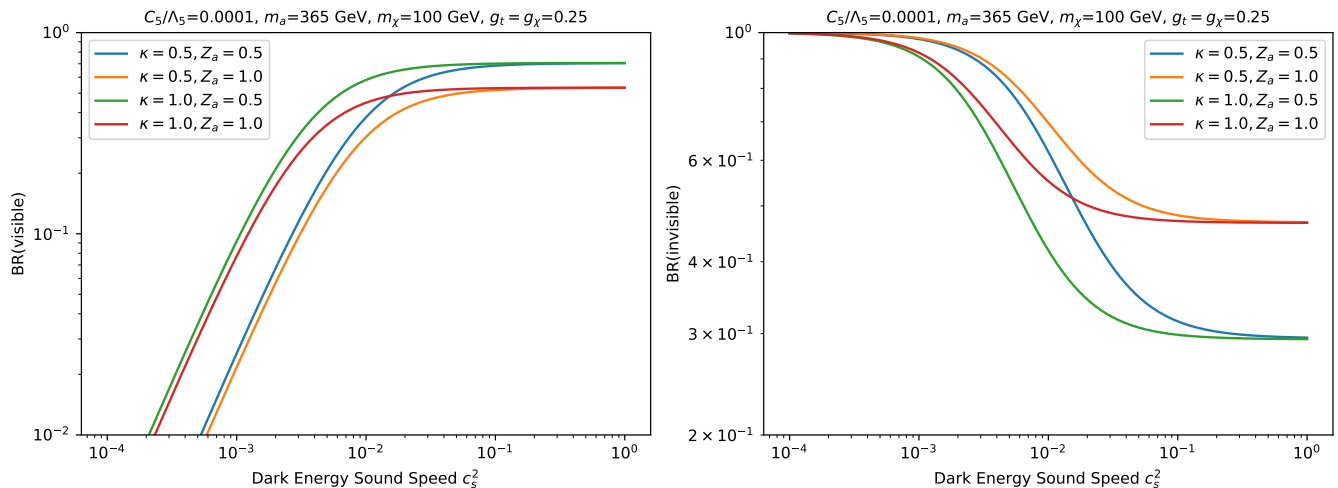
Branching Ratios of  $a \rightarrow$  visible and  $a \rightarrow$  invisible channels versus  $c_s^2$ 

FIG. 2: Branching ratios of the visible and invisible decay channels of  $a$ , defined by Eq. (65) and Eq. (66), versus  $c_s^2$ . The four curves in each of the three plots vary the parameters  $\kappa$  and  $Z_a$  as shown in the legend.

reference against which the effects of nontrivial dark energy dynamics can be assessed. Comparing the black and blue histograms, or equivalently the green and orange histograms, demonstrates that reducing  $Z_a$  from unity shifts the distribution toward larger  $p_T$  values while also introducing some broadening. This behavior reflects the increase in the physical mediator mass predicted by Eq. (15). In contrast, decreasing  $c_s^2$  primarily broadens the distribution without significantly shifting its peak position, as can be seen by comparing the black (baseline) and green histograms or the blue and orange histograms. The orange distribution, corresponding to simultaneously reduced  $c_s^2$  and  $Z_a$ , exhibits the most pronounced broadening. From an experimental perspective, these results suggest that dark energy microphysics can leave observable imprints on collider kinematic distributions. In particular, sufficiently small values of  $c_s^2$  can generate resonance shapes that depart noticeably from the narrow-width approximation and standard Breit–Wigner expectations. Although the present study is based on a simplified parton-level analysis that neglects effects such as initial-state radiation, top-quark decays, parton showering, and detector reconstruction, the qualitative trends are clear: variations in either the normalization parameter  $Z_a$  or the sound speed  $c_s^2$  can produce substantial distortions in the observed top-quark  $p_T$  spectrum. These findings highlight the potential of precision collider measurements not only to discover new mediators, but also to probe the propagation properties and underlying microphysics of the dark energy field itself.

Taken together, these results demonstrate that collider measurements of mediator widths and kinematics can probe the propagation properties of dark energy fluctuations. In particular, the dependence on  $c_s^2$  provides a direct window into the microphysics of dark energy, estab-

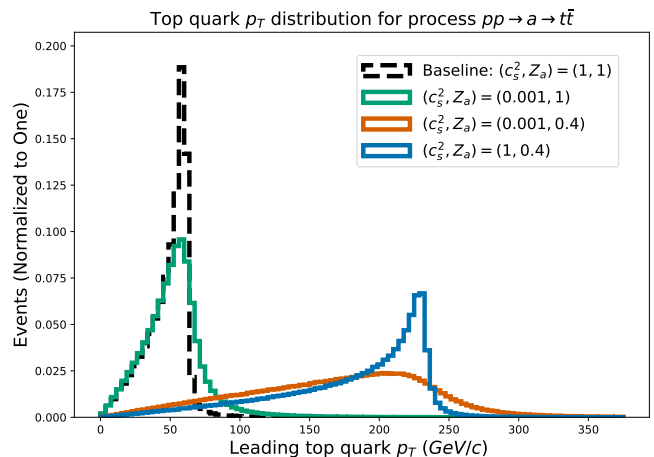


FIG. 3: Histograms of the transverse momentum of a final state top quark for the process indicated, with events normalized to one. The four curves correspond to different combinations of  $(c_s^2, Z_a)$ , with the curve in black serving as the baseline scenario with  $C_5/\Lambda_5 = 0$ .

lishing a novel and quantitative connection between high-energy collider experiments and cosmological dynamics.

## VI. DISCUSSION AND CONCLUSIONS

In this work we have developed a unified effective-field-theory framework in which collider measurements of BSM mediator resonances provide a direct probe of dark energy microphysics. By embedding a dynamical dark energy scalar sector into the 2HDM+ $a$  model through symmetry-motivated derivative interactions, we

have shown that the properties of a pseudoscalar mediator resonance—its decay widths, branching ratios, and kinematic structure—can become sensitive to parameters that are traditionally associated with cosmological dynamics.

A central result of this work is that BSM mediator observables at colliders encode information about three key quantities that characterize dark energy microphysics. First, the kinetic normalization factor  $Z_a$ , induced by higher-dimensional operators, captures the influence of the background dark energy kinetic density on the propagation and normalization of the mediator field. This effect leads to correlated shifts in the physical mediator mass, couplings, and kinematic thresholds, thereby modifying resonance lineshapes in a way that is directly testable in collider experiments. Second, the parameter  $\kappa = P_X$  controls the normalization of dark energy fluctuations and enters the decay widths through inverse powers, implying that even  $\mathcal{O}(1)$  variations can produce parametrically distinct collider signatures. Third, and most importantly, the sound speed of dark energy  $c_s^2$  governs the propagation of fluctuations and introduces a characteristic dependence in the invisible decay width through both the matrix element and the modified phase-space measure. The resulting scaling,  $(1 + c_s^2)^2/c_s^3$ , implies that subluminal sound speeds can significantly enhance invisible decay channels and alter the observable properties of the mediator resonance.

These results highlight a particularly important and timely opportunity. While cosmological observations have constrained the dark energy equation-of-state parameter  $w$  with impressive precision [52], this constraint alone does not uniquely determine the underlying microphysics [50, 51]. A wide range of theoretically distinct models – including canonical quintessence, k-essence, coupled dark energy, and more exotic scenarios – can produce nearly identical expansion histories characterized by similar values of  $w$ . In contrast, the sound speed  $c_s^2$  provides a far more discriminating observable, as it directly controls the clustering and propagation properties of dark energy perturbations. However,  $c_s^2$  remains only weakly constrained by current cosmological and astrophysical probes, which are primarily sensitive to integrated effects over large scales and long times.

In this context, collider measurements of BSM mediator resonances offer a qualitatively new and complementary probe, being sensitive to the local behavior of dark energy fluctuations through direct couplings to mediator fields. As demonstrated in this work, the dependence of decay widths and kinematics on  $c_s^2$  provides a novel pathway to access this otherwise elusive parameter. This establishes the possibility that precision measurements of BSM mediator resonances at colliders like the LHC could discriminate between different classes of dark energy models that are otherwise indistinguishable at the

level of background cosmology. More generally, we reveal a deep connection between BSM physics at colliders and the microphysical origin of cosmic acceleration, an intersection of physics which is largely uncharted as of now.

The implications of this framework extend beyond collider phenomenology. The same interactions that modify mediator properties at colliders can influence a wide range of cosmological and astrophysical phenomena. For example, the coupling between dark energy dynamics and additional fields may affect the evolution of early-Universe phase transitions, potentially altering the spectrum of stochastic gravitational-wave backgrounds accessible to current and future experiments. Furthermore, the derivative structure introduced here provides a concrete field-theoretic realization of energy exchange between dark matter and dark energy, a possibility that has been extensively explored in phenomenological studies but rarely grounded in a UV-consistent EFT framework. This opens the door to a more systematic investigation of interacting dark-sector models from first principles.

Looking ahead, our results motivate a broad and interdisciplinary research program. On the theoretical side, it will be important to explore ultraviolet completions, investigate the interplay with screening mechanisms, and extend the analysis to other classes of dark energy EFTs. On the experimental side, we emphasize that precision studies of BSM mediator resonances represent a promising and largely unexplored avenue for probing dark energy microphysics. To date, collider searches have not been interpreted within this context, and the possibility that resonance measurements could encode information about cosmic acceleration remains largely untapped.

We therefore strongly encourage the collider physics community to pursue this direction. Dedicated analyses targeting deviations in resonance lineshapes, branching ratios, and missing-energy signatures could provide the first experimental constraints on the sound speed and kinetic structure of dark energy. The prospect that measurements of BSM mediator resonances at the highest achievable energies could shed light on the physics driving the accelerated expansion of the Universe represents a compelling and unifying goal, bridging cosmology and particle physics in a fundamentally new way.

**Acknowledgements:** A.G. and C.B. gratefully acknowledge support from Vanderbilt University and the U.S. National Science Foundation. This work is supported in part by NSF Award PHY-2411502. A.F. and C.R. would like to thank the constant and enduring financial support received for this project from the Physics Department and the Faculty of Science at Universidad de Los Andes (Bogotá, Colombia). The authors would like to thank Denis Rathjens for fruitful discussions and valuable suggestions related to this work.

- [1] A. G. e. a. Riess, Observational evidence from supernovae for an accelerating universe and a cosmological constant, *Astron. J.* **116**, 1009 (1998).
- [2] S. e. a. Perlmutter, Measurements of omega and lambda from 42 high-redshift supernovae, *Astrophys. J.* **517**, 565 (1999).
- [3] D. H. Weinberg, M. J. Mortonson, D. J. Eisenstein, C. Hirata, A. G. Riess, and E. Rozo, Observational probes of cosmic acceleration, *Phys. Rept.* **530**, 87 (2013).
- [4] E. J. Copeland, M. Sami, and S. Tsujikawa, Dynamics of dark energy, *Int. J. Mod. Phys. D* **15**, 1753 (2006).
- [5] L. Amendola and S. Tsujikawa, *Dark Energy: Theory and Observations* (Cambridge University Press, 2010).
- [6] ATLAS Collaboration, Observation of a new particle in the search for the standard model higgs boson with the atlas detector at the lhc, *Phys. Lett. B* **716**, 1 (2012).
- [7] CMS Collaboration, Observation of a new boson at a mass of 125 gev with the cms experiment at the lhc, *Phys. Lett. B* **716**, 30 (2012).
- [8] S. M. Carroll, Quintessence and the rest of the world: Suppressing long-range interactions, *Phys. Rev. Lett.* **81**, 3067 (1998).
- [9] P. G. Ferreira and M. Joyce, Cosmology with a primordial scaling field, *Phys. Rev. D* **58**, 023503 (1998).
- [10] C. Burrage and J. Sakstein, Tests of chameleon gravity, *Living Rev. Relativ.* **21**, 1 (2018).
- [11] P. Brax, C. van de Bruck, A.-C. Davis, J. Khoury, and A. Weltman, Detecting dark energy in orbit: The cosmological chameleon, *Phys. Rev. D* **70**, 123518 (2004).
- [12] A. G. Riess *et al.* (Supernova Search Team), Observational evidence from supernovae for an accelerating universe and a cosmological constant, *Astron. J.* **116**, 1009 (1998), arXiv:astro-ph/9805201.
- [13] O. Avsajanishvili, G. Y. Chitov, T. Kahniashvili, S. Mandal, and L. Samushia, Observational Constraints on Dynamical Dark Energy Models, *Universe* **2024**, 10.3390/universe10030122 (2024), arXiv:2310.16911 [astro-ph.CO].
- [14] M. Li, X.-D. Li, S. Wang, and Y. Wang, Dark Energy: A Brief Review, *Front. Phys. (Beijing)* **8**, 828 (2013), arXiv:1209.0922 [astro-ph.CO].
- [15] M. Li, X.-D. Li, S. Wang, and Y. Wang, Dark Energy, *Commun. Theor. Phys.* **56**, 525 (2011), arXiv:1103.5870 [astro-ph.CO].
- [16] M. J. Mortonson, D. H. Weinberg, and M. White, Dark Energy: A Short Review (2013), arXiv:1401.0046 [astro-ph.CO].
- [17] D. Huterer and D. L. Shafer, Dark energy two decades after: Observables, probes, consistency tests, *Rept. Prog. Phys.* **81**, 016901 (2018), arXiv:1709.01091 [astro-ph.CO].
- [18] C. Cheung, P. Creminelli, A. L. Fitzpatrick, J. Kaplan, and L. Senatore, The Effective Field Theory of Inflation, *JHEP* **03**, 014, arXiv:0709.0293 [hep-th].
- [19] G. Gubitosi, F. Piazza, and F. Vernizzi, The effective field theory of dark energy, *Journal of Cosmology and Astroparticle Physics* **2013** (02), 032.
- [20] S. Vagnozzi, L. Visinelli, P. Brax, A.-C. Davis, and J. Sakstein, Direct detection of dark energy: The XENON1T excess and future prospects, *Phys. Rev. D* **104**, 063023 (2021), arXiv:2103.15834 [hep-ph].
- [21] S. A. Adil, U. Mukhopadhyay, A. A. Sen, and S. Vagnozzi, Dark energy in light of the early JWST observations: case for a negative cosmological constant?, *JCAP* **10**, 072, arXiv:2307.12763 [astro-ph.CO].
- [22] E. Di Valentino, S. Gariazzo, O. Mena, and S. Vagnozzi, Soundness of Dark Energy properties, *JCAP* **07** (07), 045, arXiv:2005.02062 [astro-ph.CO].
- [23] S. Nojiri and S. D. Odintsov, Unified cosmic history in modified gravity: from F(R) theory to Lorentz non-invariant models, *Phys. Rept.* **505**, 59 (2011), arXiv:1011.0544 [gr-qc].
- [24] S. Nojiri and S. D. Odintsov, Introduction to modified gravity and gravitational alternative for dark energy, *eConf C0602061*, 06 (2006), arXiv:hep-th/0601213.
- [25] B. Gumjudpai, T. Naskar, M. Sami, and S. Tsujikawa, Coupled dark energy: towards a general description of the dynamics, *Journal of Cosmology and Astroparticle Physics* **2005** (06), 007.
- [26] A. Gómez-Valent, V. Pettorino, and L. Amendola, Update on coupled dark energy and the h 0 tension, *Physical Review D* **101**, 123513 (2020).
- [27] B. J. Barros, Kinetically coupled dark energy, *Physical Review D* **99**, 064051 (2019).
- [28] J.-Q. Xia, Constraint on coupled dark energy models from observations, *Physical Review D—Particles, Fields, Gravitation, and Cosmology* **80**, 103514 (2009).
- [29] A. V. Macciò, C. Quercellini, R. Mainini, L. Amendola, and S. A. Bonometto, Coupled dark energy: Parameter constraints from n-body simulations, *Physical Review D* **69**, 123516 (2004).
- [30] C. Armendariz-Picon, V. Mukhanov, and P. J. Steinhardt, Essentials of k-essence, *Physical Review D* **63**, 103510 (2001).
- [31] M. Malquarti, E. J. Copeland, A. R. Liddle, and M. Trodden, A new view of k-essence, *Physical Review D* **67**, 123503 (2003).
- [32] C. Armendariz-Picon and E. A. Lim, Haloes of k-essence, *Journal of Cosmology and Astroparticle Physics* **2005** (08), 007.
- [33] C. Ahn, C. Kim, and E. V. Linder, Dark energy properties in dbi theory, *Physical Review D—Particles, Fields, Gravitation, and Cosmology* **80**, 123016 (2009).
- [34] L. P. Chimento, R. Lazkoz, and I. Sendra, Dbi models for the unification of dark matter and dark energy, *General Relativity and Gravitation* **42**, 1189 (2010).
- [35] R.-G. Cai and S.-J. Wang, Dark matter superfluid and dbi dark energy, *Physical Review D* **93**, 023515 (2016).
- [36] S. Chattopadhyay and U. Debnath, Interaction between dbi-essence and other dark energies, *International Journal of Theoretical Physics* **49**, 1465 (2010).
- [37] G. Calcagni and A. R. Liddle, Tachyon dark energy models: Dynamics and constraints, *Physical Review D—Particles, Fields, Gravitation, and Cosmology* **74**, 043528 (2006).
- [38] J. Bagla, H. K. Jassal, and T. Padmanabhan, Cosmology with tachyon field as dark energy, *Physical Review D* **67**, 063504 (2003).
- [39] E. J. Copeland, M. R. Garousi, M. Sami, and S. Tsujikawa, What is needed of a tachyon if it is to be the dark energy?, *Physical Review D—Particles, Fields, Gravita-*

- tion, and Cosmology **71**, 043003 (2005).
- [40] S. M. Micheletti, Observational constraints on holographic tachyonic dark energy in interaction with dark matter, *Journal of Cosmology and Astroparticle Physics* **2010** (05), 009.
- [41] A. Sheykhi, M. Sadegh Movahed, and E. Ebrahimi, Tachyon reconstruction of ghost dark energy, *Astrophysics and Space Science* **339**, 93 (2012).
- [42] J. Kehayias and R. J. Scherrer, New generic evolution for  $k$ -essence dark energy with  $w \approx -1$ , *Phys. Rev. D* **100**, 023525 (2019), arXiv:1905.05628 [gr-qc].
- [43] T. Chiba, S. Dutta, and R. J. Scherrer, Slow-roll  $k$ -essence, *Phys. Rev. D* **80**, 043517 (2009), arXiv:0906.0628 [astro-ph.CO].
- [44] R. Das, T. W. Kephart, and R. J. Scherrer, Tracking quintessence and  $k$ -essence in a general cosmological background, *Phys. Rev. D* **74**, 103515 (2006), arXiv:gr-qc/0609014.
- [45] N. Frusciante and L. Perenon, Effective field theory of dark energy: A review, *Phys. Rept.* **857**, 1 (2020), arXiv:1907.03150 [astro-ph.CO].
- [46] E. V. Linder, G. Sengör, and S. Watson, Is the effective field theory of dark energy effective?, *Journal of Cosmology and Astroparticle Physics* **2016** (05), 053.
- [47] J. Bloomfield, É. É. Flanagan, M. Park, and S. Watson, Dark energy or modified gravity? an effective field theory approach, *Journal of Cosmology and Astroparticle Physics* **2013** (08), 010.
- [48] J.-H. Liang, Y. Liao, X.-D. Ma, and H.-L. Wang, Dark sector effective field theory, *Journal of High Energy Physics* **2023**, 1 (2023).
- [49] N. Frusciante, M. Raveri, and A. Silvestri, Effective field theory of dark energy: a dynamical analysis, *Journal of Cosmology and Astroparticle Physics* **2014** (02), 026.
- [50] A. Gurrola, R. J. Scherrer, and O. Trivedi, Probing the Sound Speed of Dark Energy with a Lunar Laser Interferometer (2026), arXiv:2601.22084 [astro-ph.CO].
- [51] A. Gurrola, R. J. Scherrer, and O. Trivedi, Probing Dark Energy on the Moon (2026), arXiv:2603.04841 [astro-ph.CO].
- [52] N. Aghanim, T. Ghosh, J. J. Bock, B. P. Crill, O. Doré, S. R. Hildebrandt, G. Rocha, K. M. Górski, C. R. Lawrence, S. Mitra, G. Roudier, and P. Collaboration, Planck 2018 results. vi. cosmological parameters, *Astronomy and Astrophysics* **641**, Art. No. A6 (2020).
- [53] S. Hannestad, Constraints on the sound speed of dark energy, *Phys. Rev. D* **71**, 103519 (2005), arXiv:astro-ph/0504017.
- [54] R. de Putter, D. Huterer, and E. V. Linder, Measuring the speed of dark: Detecting dark energy perturbations, *Physical Review D—Particles, Fields, Gravitation, and Cosmology* **81**, 103513 (2010).
- [55] G. Ballesteros and J. Lesgourgues, Dark energy with non-adiabatic sound speed: initial conditions and detectability, *Journal of Cosmology and Astroparticle Physics* **2010** (10), 014.
- [56] M. S. Linton, A. Pourtsidou, R. Crittenden, and R. Maartens, Variable sound speed in interacting dark energy models, *Journal of Cosmology and Astroparticle Physics* **2018** (04), 043.
- [57] R. Bean and O. Dore, Probing dark energy perturbations: the dark energy equation of state and speed of sound as measured by wmap, *Physical Review D* **69**, 083503 (2004).
- [58] D. J. Eisenstein, Dark energy and cosmic sound, *New Astronomy Reviews* **49**, 360 (2005).
- [59] O. Sergijenko and B. Novosyadlyj, Sound speed of scalar field dark energy: weak effects and large uncertainties, *Physical Review D* **91**, 083007 (2015).
- [60] Y.-F. Shen, A. Gurrola, F. Romeo, D. Rathjens, and A. Flórez, Heavy Neutrinos across the Electroweak-to-Multi-TeV Frontier via Novel ML-Enhanced Probes (2026), arXiv:2601.09095 [hep-ph].
- [61] Y.-F. Shen and A. Gurrola, Large-Width New Physics at Colliders: A Gauge-Invariant Resummation Approach (2025), arXiv:2511.15114 [hep-ph].
- [62] U. S. Qureshi, A. Gurrola, and A. Flórez, Probing compressed mass spectrum supersymmetry at the high-luminosity LHC with the vector boson fusion topology, *Eur. Phys. J. C* **85**, 1208 (2025), arXiv:2411.13837 [hep-ph].
- [63] U. S. Qureshi, A. Gurrola, A. Flórez, and C. Rodriguez, Probing light scalars and vector-like quarks at the high-luminosity LHC, *Eur. Phys. J. C* **85**, 379 (2025), arXiv:2410.17854 [hep-ph].
- [64] D. Barbosa, F. Díaz, L. Quintero, A. Flórez, M. Sanchez, A. Gurrola, E. Sheridan, and F. Romeo, Probing a  $Z'$  with non-universal fermion couplings through top quark fusion, decays to bottom quarks, and machine learning techniques, *Eur. Phys. J. C* **83**, 413 (2023), arXiv:2210.15813 [hep-ph].
- [65] A. Gurrola and J. D. Ruiz-Álvarez, Quarkophobic  $W'$  for LHC searches, in *20th Conference on Flavor Physics and CP Violation* (2022) arXiv:2208.01861 [hep-ph].
- [66] B. Dutta, S. Ghosh, A. Gurrola, D. Julson, T. Kamon, and J. Kumar, Probing an MeV-scale scalar boson in association with a TeV-Scale top-quark partner at the LHC, *JHEP* **03**, 164, arXiv:2202.08234 [hep-ph].
- [67] N. Cardona, F. Andrés, G. Alfredo, J. Will, S. Paul, and T. Cheng, Long-term LHC discovery reach for compressed Supersymmetry models using VBF processes, *JHEP* **11**, 026, arXiv:2102.10194 [hep-ph].
- [68] A. Flórez, A. Gurrola, W. Johns, P. Sheldon, E. Sheridan, K. Sinha, and B. Soubasis, Probing axionlike particles with  $\gamma\gamma$  final states from vector boson fusion processes at the LHC, *Phys. Rev. D* **103**, 095001 (2021), arXiv:2101.11119 [hep-ph].
- [69] A. Flórez, A. Gurrola, W. Johns, J. Maruri, P. Sheldon, K. Sinha, and S. R. Starko, Anapole Dark Matter via Vector Boson Fusion Processes at the LHC, *Phys. Rev. D* **100**, 016017 (2019), arXiv:1902.01488 [hep-ph].
- [70] A. Flórez, Y. Guo, A. Gurrola, W. Johns, O. Ray, P. Sheldon, and S. Starko, Probing heavy spin-2 bosons with  $\gamma\gamma$  final states from vector boson fusion processes at the LHC, *Phys. Rev. D* **99**, 035034 (2019), arXiv:1812.06824 [hep-ph].
- [71] R. Leonardi, O. Panella, F. Romeo, A. Gurrola, H. Sun, and S.-S. Xue, Phenomenology at the LHC of composite particles from strongly interacting Standard Model fermions via four-fermion operators of NJL type, *Eur. Phys. J. C* **80**, 309 (2020), arXiv:1810.11420 [hep-ph].
- [72] C. Avila, A. Flórez, A. Gurrola, D. Julson, and S. Starko, Connecting particle physics and cosmology: Measuring the dark matter relic density in compressed supersymmetry models at the LHC, *Phys. Dark Univ.* **27**, 100430 (2020), arXiv:1801.03966 [hep-ph].

- [73] A. Flórez, K. Gui, A. Gurrola, C. Patiño, and D. Restrepo, Expanding the Reach of Heavy Neutrino Searches at the LHC, *Phys. Lett. B* **778**, 94 (2018), arXiv:1708.03007 [hep-ph].
- [74] A. Flórez, A. Gurrola, W. Johns, Y. D. Oh, P. Sheldon, D. Teague, and T. Weiler, Searching for New Heavy Neutral Gauge Bosons using Vector Boson Fusion Processes at the LHC, *Phys. Lett. B* **767**, 126 (2017), arXiv:1609.09765 [hep-ph].
- [75] A. Flórez, L. Bravo, A. Gurrola, C. Ávila, M. Segura, P. Sheldon, and W. Johns, Probing the stau-neutralino coannihilation region at the LHC with a soft tau lepton and a jet from initial state radiation, *Phys. Rev. D* **94**, 073007 (2016), arXiv:1606.08878 [hep-ph].
- [76] B. Dutta, A. Gurrola, K. Hatakeyama, W. Johns, T. Kamon, P. Sheldon, K. Sinha, S. Wu, and Z. Wu, Probing Compressed Bottom Squarks with Boosted Jets and Shape Analysis, *Phys. Rev. D* **92**, 095009 (2015), arXiv:1507.01001 [hep-ph].
- [77] B. Dutta, T. Ghosh, A. Gurrola, W. Johns, T. Kamon, P. Sheldon, K. Sinha, K. Wang, and S. Wu, Probing Compressed Sleptons at the LHC using Vector Boson Fusion Processes, *Phys. Rev. D* **91**, 055025 (2015), arXiv:1411.6043 [hep-ph].
- [78] B. Dutta, W. Flanagan, A. Gurrola, W. Johns, T. Kamon, P. Sheldon, K. Sinha, K. Wang, and S. Wu, Probing compressed top squark scenarios at the LHC at 14 TeV, *Phys. Rev. D* **90**, 095022 (2014), arXiv:1312.1348 [hep-ph].
- [79] B. Dutta, A. Gurrola, W. Johns, T. Kamon, P. Sheldon, and K. Sinha, Vector Boson Fusion Processes as a Probe of Supersymmetric Electroweak Sectors at the LHC, *Phys. Rev. D* **87**, 035029 (2013), arXiv:1210.0964 [hep-ph].
- [80] B. Dutta, A. Gurrola, T. Kamon, A. Krislock, A. B. Lahanas, N. E. Mavromatos, and D. V. Nanopoulos, Supersymmetry Signals of Supercritical String Cosmology at the Large Hadron Collider, *Phys. Rev. D* **79**, 055002 (2009), arXiv:0808.1372 [hep-ph].
- [81] R. L. Arnowitt, B. Dutta, A. Gurrola, T. Kamon, A. Krislock, and D. Toback, Determining the Dark Matter Relic Density in the mSUGRA ( $\tilde{\chi}_0(1)$ )- $\tau$  Co-Annihilation Region at the LHC, *Phys. Rev. Lett.* **100**, 231802 (2008), arXiv:0802.2968 [hep-ph].
- [82] A. G. Delannoy *et al.*, Probing Dark Matter at the LHC using Vector Boson Fusion Processes, *Phys. Rev. Lett.* **111**, 061801 (2013), arXiv:1304.7779 [hep-ph].
- [83] G. C. Branco, P. M. Ferreira, L. Lavoura, M. N. Rebelo, M. Sher, and J. P. Silva, Theory and phenomenology of two-Higgs-doublet models, *Phys. Rept.* **516**, 1 (2012), arXiv:1106.0034 [hep-ph].
- [84] N. Craig, J. Galloway, and S. Thomas, Searching for Signs of the Second Higgs Doublet (2013), arXiv:1305.2424 [hep-ph].
- [85] J. F. Gunion and H. E. Haber, The CP conserving two Higgs doublet model: The Approach to the decoupling limit, *Phys. Rev. D* **67**, 075019 (2003), arXiv:hep-ph/0207010.
- [86] D. Abercrombie *et al.*, Dark Matter benchmark models for early LHC Run-2 Searches: Report of the ATLAS/CMS Dark Matter Forum, *Phys. Dark Univ.* **27**, 100371 (2020), arXiv:1507.00966 [hep-ex].
- [87] J. Abdallah *et al.*, Simplified Models for Dark Matter Searches at the LHC, *Phys. Dark Univ.* **9-10**, 8 (2015), arXiv:1506.03116 [hep-ph].
- [88] A. Boveia and C. Doglioni, Dark Matter Searches at Colliders, *Ann. Rev. Nucl. Part. Sci.* **68**, 429 (2018), arXiv:1810.12238 [hep-ex].
- [89] G. Aad *et al.* (ATLAS), Observation of a cross-section enhancement near the  $t\bar{t}$  production threshold in  $\sqrt{s} = 13$  TeV  $pp$  collisions with the ATLAS detector (2026), arXiv:2601.11780 [hep-ex].
- [90] A. Hayrapetyan *et al.* (CMS), Observation of a pseudoscalar excess at the top quark pair production threshold, *Rept. Prog. Phys.* **88**, 087801 (2025), arXiv:2503.22382 [hep-ex].
- [91] M. Bauer, U. Haisch, and F. Kahlhoefer, Simplified dark matter models with two higgs doublets: I. pseudoscalar mediators, *JHEP* **05**, 138, arXiv:1701.07427 [hep-ph].
- [92] M. Bauer, U. Haisch, and F. Kahlhoefer, Simplified dark matter models with two higgs doublets: II. phenomenology and constraints, *JHEP* **05**, 103, arXiv:1701.07427 [hep-ph].
- [93] J. M. No, Looking for higgs portal dark matter with mono-higgs signatures at the lhc, *Phys. Rev. D* **93**, 031701 (2016), arXiv:1509.01110 [hep-ph].
- [94] C. Arina, M. Backovic, J. Heisig, F. Maltoni, and M. Pellen, A comprehensive analysis of dark matter models with pseudoscalar mediators, *JHEP* **11**, 111, arXiv:1605.09242 [hep-ph].
- [95] G. Arcadi, N. Benincasa, A. Djouadi, and K. Kannike, Two-higgs-doublet-plus-pseudoscalar model: Collider, dark matter, and gravitational wave signals, *Physical Review D* **108**, 055010 (2023).
- [96] G. Arcadi, M. Dutra, P. Ghosh, M. Lindner, Y. Mambrini, M. Pierre, S. Profumo, and F. S. Queiroz, The waning of the wimp? a review of models, searches, and constraints, *Eur. Phys. J. C* **78**, 203 (2018), arXiv:1703.07364 [hep-ph].
- [97] T. B. Vasilev, M. Bouhmadi-López, and P. Martín-Moruno, Dark energy with a shift-symmetric scalar field: Obstacles, loophole hunting and dead ends, *Physics of the Dark Universe* **46**, 101679 (2024), arXiv:2406.12576 [gr-qc].
- [98] C. Deffayet, O. Pujolàs, I. Sawiki, and A. Vikman, Imperfect dark energy from kinetic gravity braiding, *Journal of Cosmology and Astroparticle Physics* **2010**, arXiv:1008.0048 [hep-th].
- [99] C. Armendariz-Picon, T. Damour, and V. Mukhanov, k-inflation, *Phys. Lett. B* **458**, 209 (1999), hep-th/9904075.
- [100] J. Garriga and V. F. Mukhanov, Perturbations in k-inflation, *Phys. Lett. B* **458**, 219 (1999), hep-th/9904176.
- [101] S. Tsujikawa, Quintessence: A review (2013), arXiv:1304.1961 [gr-qc].
- [102] B. Ratra and P. J. E. Peebles, Cosmological consequences of a rolling homogeneous scalar field, *Phys. Rev. D* **37**, 3406 (1988).
- [103] R. R. Caldwell, R. Dave, and P. J. Steinhardt, Cosmological imprint of an energy component with general equation of state, *Phys. Rev. Lett.* **80**, 1582 (1998), astro-ph/9708069.
- [104] C. Armendariz-Picon, V. Mukhanov, and P. J. Steinhardt, A dynamical solution to the problem of a small cosmological constant and late time cosmic acceleration, *Phys. Rev. Lett.* **85**, 4438 (2000), astro-ph/0004134.

- [105] S. DeDeo, R. R. Caldwell, and P. J. Steinhardt, Effects of the sound speed of quintessence on the microwave background and large scale structure, *Phys. Rev. D* **67**, 103509 (2003), astro-ph/0301284.
- [106] W. Hu, Structure Formation with Generalized Dark Matter, *Astrophys. J.* **506**, 485 (1998), arXiv:astro-ph/9801234.
- [107] J. K. Erickson, R. R. Caldwell, P. J. Steinhardt, C. Armendariz-Picon, and V. Mukhanov, Measuring the speed of sound of quintessence, *Phys. Rev. Lett.* **88**, 121301 (2002), astro-ph/0112438.
- [108] M. Berbig, Kick it like DESI: PNGB quintessence with a dynamically generated initial velocity, *Journal of Cosmology and Astroparticle Physics* arXiv:2412.07418 [astro-ph.CO].
- [109] C.-I. Chiang and H. Murayama, Building Supergravity Quintessence Model, arXiv preprint arXiv:1808.02279 (2018).
- [110] B. Finelli, G. Goon, E. Pajer, and L. Santoni, The effective theory of shift-symmetric cosmologies, *Journal of Cosmology and Astroparticle Physics* **2018**, arXiv:1802.01580 [hep-th].
- [111] K. Kaneta, S. M. Lee, K.-y. Oda, and T. Takahashi, Pseudo-Nambu-Goldstone boson production from inflation coupling during reheating, *Journal of Cosmology and Astroparticle Physics* **2024**, arXiv:2406.09045 [astro-ph].
- [112] P. Sikivie, Experimental tests of the invisible axion, *Phys. Rev. Lett.* **51**, 1415 (1983).
- [113] J. E. Kim, Light pseudoscalars, particle physics and cosmology, *Phys. Rept.* **150**, 1 (1987).
- [114] D. J. E. Marsh, Axion cosmology (2016), arXiv:1510.07633 [astro-ph.CO].
- [115] J. M. Ziman, *Electrons and Phonons: The Theory of Transport Phenomena in Solids* (Oxford University Press, 1960).
- [116] C. Kittel, *Introduction to Solid State Physics*, 8th ed. (Wiley, 2004).
- [117] E. Braaten and R. D. Pisarski, Soft amplitudes in hot gauge theories: A general analysis, *Nucl. Phys. B* **337**, 569 (1990).
- [118] J. I. Kapusta and C. Gale, *Finite-Temperature Field Theory: Principles and Applications*, 2nd ed. (Cambridge University Press, 2006).
- [119] V. F. Mukhanov, H. A. Feldman, and R. H. Brandenberger, *Theory of cosmological perturbations*, Vol. 215 (1992) pp. 203–333.
- [120] S. Weinberg, *Cosmology* (Oxford University Press, 2008).
- [121] A. Hayrapetyan *et al.* (CMS), Dark sector searches with the CMS experiment, *Phys. Rept.* **1115**, 448 (2025), arXiv:2405.13778 [hep-ex].
- [122] J. Alwall *et al.*, The automated computation of tree-level and next-to-leading order differential cross sections, and their matching to parton shower simulations, *Journal of High Energy Physics* **2014**, 10.1007/JHEP07(2014)079 (2014), arXiv:1405.0301 [hep-ph].
- [123] E. Conte, B. Fuks, and G. Serret, MADANALYSIS 5, a user-friendly framework for collider phenomenology, *Computer Physics Communications* **184**, 10.1016/j.cpc.2012.09.009 (2013), arXiv:1206.1599 [hep-ph].